the current study. Finally, interferon therapy may affect albuminuria and renal function, which may be either reversible or irreversible.[28–30] Although information on the history of interferon therapy was not available in the current study, this point should be taken into account in future studies.

CONCLUSION

IN CONCLUSION, BY analyzing the cross-sectional data of 12 535 individuals who underwent general health screening, we have investigated a possible association between viral hepatitis infection and CKD components. There was a positive association between HCcAg positivity, but not HBsAg positivity, and CKD components (low eGFR and albuminuria). The observed associations were confounded by the degree of insulin resistance and serum ALT levels. Although HCcAg positivity was associated with increased insulin resistance, HCcAg positivity was negatively associated with metabolic syndrome. These data collectively indicate that some differences may exist between HCV infection and HBV infection in terms of association with CKD components in Japanese individuals who undergo general health screening.

ACKNOWLEDGMENTS

THIS WORK WAS supported in part by grants from the Smoking Research Foundation, Chiyoda Mutual Life Foundation, St Luke's Grant for the Epidemiological Research and Daiwa Securities Health Foundation.

REFERENCES

1 Higuchi M, Tanaka E, Kiyosawa K. Epidemiology and clinical aspects on hepatitis C. *Jpn J Infect Dis* 2002; **55**: 69–77.
2 Narai R, Oyama T, Ogawa M *et al.* HBV- and HCV- infected workers in the Japanese workplace. *J Occup Health* 2007; **49**: 9–16.
3 Yamabe H, Johnson RJ, Gretch DR *et al.* Hepatitis C virus infection and membranoproliferative glomerulonephritis in Japan. *J Am Soc Nephrol* 1995; **6**: 220–3.
4 El-Serag HB, Hampel H, Yeh C, Rabeneck L. Extrahepatic manifestations of hepatitis C among United States male veterans. *Hepatology* 2002; **36**: 1439–45.
5 Johnson RJ, Couser WG. Hepatitis B infection and renal disease: clinical, immunopathogenetic and therapeutic considerations. *Kidney Int* 1990; **37**: 663–76.
6 Tang S, Lai FM, Lui YH *et al.* Lamivudine in hepatitis B-associated membranous nephropathy. *Kidney Int* 2005; **68**: 1750–8.
7 Cacoub P, Saadoun D, Bourliere M *et al.* Hepatitis B virus genotypes and extrahepatic manifestations. *J Hepatol* 2005; **43**: 764–70.
8 Tsui JI, Vittinghoff E, Shlipak MG, O'Hare AM. Relationship between hepatitis C and chronic kidney disease: results from the Third National Health and Nutrition Examination Survey. *J Am Soc Nephrol* 2006; **17**: 1168–74.
9 Manjunath G, Samak MJ, Levey AS. Prediction equations to estimate glomerular filtration rate: an update. *Curr Opin Nephrol Hypertens* 2001; **10**: 785–92.
10 Imai E, Horio M, Nitta K *et al.* Estimation of glomerular filtration rate by the MDRD study equation modified for Japanese patients with chronic kidney disease. *Clin Exp Nephrol* 2007; **11**: 41–50.
11 National Kidney Foundation. K/DOQI clinical practice guidelines for chronic kidney disease: evaluation, classification, and stratification. *Am J Kidney Dis* 2002; **39**: S1–266.
12 Alberti KG, Zimmet PZ. Definition, diagnosis and classification of diabetes mellitus and its complications. Part 1: diagnosis and classification of diabetes mellitus provisional report of a WHO consultation. *Diabet Med* 1998; **15**: 539–53.
13 Ishizaka N, Ishizaka Y, Toda E, Nagai R, Yamakado M. Association between serum uric acid, metabolic syndrome, and carotid atherosclerosis in Japanese individuals. *Arterioscler Thromb Vasc Biol* 2005; **25**: 1038–44.
14 Moriya K, Shintani Y, Fujie H *et al.* Serum lipid profile of patients with genotype 1b hepatitis C viral infection in Japan. *Hepatol Res* 2003; **25**: 371–6.
15 Serfaty L, Andreani T, Giral P, Carbonell N, Chazouilleres O, Poupon R. Hepatitis C virus induced hypobetalipoproteinemia: a possible mechanism for steatosis in chronic hepatitis C. *J Hepatol* 2001; **34**: 428–34.
16 Combes B, Shorey J, Barrera A *et al.* Glomerulonephritis with deposition of Australia antigen-antibody complexes in glomerular basement membrane. *Lancet* 1971; **2**: 234–7.
17 Huang JF, Chuang WL, Dai CY *et al.* Viral hepatitis and proteinuria in an area endemic for hepatitis B and C infections: another chain of link? *J Intern Med* 2006; **260**: 255–62.
18 Tai TY, Lu JY, Chen CL *et al.* Interferon-alpha reduces insulin resistance and beta-cell secretion in responders among patients with chronic hepatitis B and C. *J Endocrinol* 2003; **178**: 457–65.
19 Shaheen M, Echeverry D, Oblad MG, Montoya MI, Teklehaimanot S, Akhtar AJ. Hepatitis C, metabolic syndrome, and inflammatory markers: results from the Third National Health and Nutrition Examination Survey [NHANES III]. *Diabetes Res Clin Pract* 2007; **75**: 320–6.
20 Shintani Y, Fujie H, Miyoshi H *et al.* Hepatitis C virus infection and diabetes: direct involvement of the virus in the development of insulin resistance. *Gastroenterology* 2004; **126**: 840–8.

21 Koike K. Hepatitis C virus infection can present with metabolic disease by inducing insulin resistance. *Intervirology* 2006; **49**: 51–7.
22 Custro N, Carroccio A, Ganci A *et al.* Glycemic homeostasis in chronic viral hepatitis and liver cirrhosis. *Diabetes Metab* 2001; **27**: 476–81.
23 Wang CC, Hsu CS, Liu CJ, Kao JH, Chen DS. Association of chronic hepatitis B virus infection with insulin resistance and hepatic steatosis. *J Gastroenterol Hepatol* 2008; (in press).
24 Niskanen L, Laakso M. Insulin resistance is related to albuminuria in patients with type II (non-insulin-dependent) diabetes mellitus. *Metabolism* 1993; **42**: 1541–5.
25 Ian CF, Chen CJ, Chiu YH *et al.* A population-based study investigating the association between metabolic syndrome and hepatitis B/C infection (Keelung Community-based Integrated Screening study, 10). *Int J Obes (Lond)* 2006; **30**: 794–9.
26 Luo B, Wang Y, Wang K. Association of metabolic syndrome and hepatitis B infection in a Chinese population. *Clin Chim Acta* 2007; **380**: 238–40.
27 Bonora E, Coscelli C, Orioli S *et al.* Hyperinsulinemia of chronic active hepatitis: impaired insulin removal rather than pancreatic hypersecretion. *Horm Metab Res* 1984; **16**: 111–14.
28 Jones GJ, Itri LM. Safety and tolerance of recombinant interferon alfa-2a (Roferon-A) in cancer patients. *Cancer* 1986; **57**: 1709–15.
29 Quesada JR, Talpaz M, Rios A, Kurzrock R, Gutterman JU. Clinical toxicity of interferons in cancer patients: a review. *J Clin Oncol* 1986; **4**: 234–43.
30 Lederer E, Truong L. Unusual glomerular lesion in a patient receiving long-term interferon alpha. *Am J Kidney Dis* 1992; **20**: 516–18.

Hepatology Research 2008; **38**: 252–258 doi: 10.1111/j.1872-034X.2007.00257.x

Original Article

Effect of treatment with interferon α-2b and ribavirin in patients infected with genotype 2 hepatitis C virus

Yoshihiko Nagase,[1] Hiroshi Yotsuyanagi,[1,2] Chiaki Okuse,[1] Kiyomi Yasuda,[3] Tomohiro Kato,[4] Kazuhiko Koike,[2] Michihiro Suzuki,[1] Kusuki Nishioka,[4] Shiro Iino[3] and Fumio Itoh[1]

[1]*Department of Internal Medicine, Division of Gastroenterology and Hepatology and* [4]*Department of Bioregulation and Proteomics, St. Marianna University, Kawasaki,* [2]*Department of Infectious Diseases, Internal Medicine, Graduate School of Medicine, University of Tokyo and* [3]*Center for Liver Diseases, Kiyokawa Hospital, Tokyo, Japan*

Aim: Nearly 20% of chronic hepatitis C (CHC) patients with genotype 2 hepatitis C virus (HCV) infection are not curable, even by interferon (IFN)–ribavirin combination therapy. The aim of this study is to investigate the factors that determine the efficacy of combination therapy in patients with genotype 2 HCV infection.

Methods: Fifty patients with CHC who underwent a treatment of 6 MU IFN α-2b with ribavirin for 24 weeks were retrospectively analyzed.

Results: All the patients showed no serum HCV-RNA within 12 weeks after starting the therapy. Forty-one of the 50 patients (82%) achieved a sustained virological response (SVR). The age, sex, genotype (2a vs. 2b) and grade/stage of the liver by histopathology and pretreatment viral load were not different between the sustained responders and relapsers. Univariate analysis showed that an earlier viral clearance from blood and a larger number of amino acid substitutions in the interferon sensitivity determining region (ISDR) were predictors of SVR. Multivariate analysis showed that a large number of amino acid substitutions in the ISDR was a predictor of SVR.

Conclusion: The characterization of the amino acid sequences of ISDR may be helpful for predicting a relapse after combination therapy in patients with genotype 2 HCV infection.

Key words: genotype, hepatitis C virus, interferon, ISDR, ribavirin

INTRODUCTION

CHRONIC HEPATITIS C (CHC) is an infection that affects more than 150 million people worldwide. Up to 50% of these people develop chronic liver disease leading to liver cirrhosis.[1–3] Once liver cirrhosis has developed, up to 7% of these patients per year develop hepatocellular carcinoma.[4–6] Antiviral treatment is crucial for the control of this disease.

Before the use of ribavirin, interferon (IFN) monotherapy was the only effective treatment for CHC. Although many clinical trials and several meta-analyses have documented the efficacy of IFN monotherapy, the rate of sustained virological response (SVR) is low, particularly in patients with genotype 1 or 4 hepatitis C virus (HCV) infection.[7–9]

The combination therapy of IFN and ribavirin has been shown to be more effective than IFN monotherapy for CHC.[10–14] The baseline level of serum HCV-RNA before treatment and HCV genotype are predictors of a SVR to IFN therapy.[15] With regard to HCV genotype, patients who are infected with genotype 2 or 3 HCV can achieve a higher SVR rate than those with genotype 1 HCV. However, even with genotype 2 HCV infection, combination therapy for 24 weeks failed to eradicate the virus in about 20% of patients,[12–14] although the reason for this is still unclear.

Besides HCV genotype and viral load, mutations in the interferon sensitivity determining region (ISDR, aa 2209–2248) of the non-structural region 5A (NS5A) of

Correspondence: Dr Hiroshi Yotsuyanagi, Department of Infectious Diseases, Internal Medicine, Graduate School of Medicine, University of Tokyo, 7-3-1 Hongo, Bunkyo-ku, Tokyo 113-8655, Japan. Email: hyotsu-tky@umin.ac.jp

Grant sponsor: Japanese Ministry of Health, Labor and Welfare.
Received 7 September 2006; revision 28 June 2007; accepted 16 July 2007.

HCV have also been reported to influence the efficacy of IFN. In genotype 1 HCV infection, the number of amino acid substitutions in ISDR is reported to be related to the efficacy of IFN therapy in Japan and Europe,[16–20] although this correlation is still controversial.[21] In genotype 2 infection, the amino acid sequence of ISDR has been reported to also correlate with SVR to IFN monotherapy.[22–24] Therefore, the efficacy of IFN–ribavirin combination therapy in genotype 2 HCV-infected patients may be determined by the amino acid sequence of ISDR, which has not yet been studied.

The aim of this study is to elucidate factors that determine the response to IFN–ribavirin combination therapy in patients with genotype 2 HCV infection.

METHODS

Patient selection

FROM 2001 TO 2003, 140 patients (84 men and 56 women; mean age, 53.8 ± 11.3 years) were treated with recombinant IFN α-2b (Intron A; Schering-Plough, Kenilworth, NJ) and ribavirin (Rebetol; Schering-Plough, Kenilworth, NJ) combination therapy. Eighty-five patients had genotype 1 HCV infection (54 men and 31 women; mean age, 56.3 ± 10.5 years) and 55 patients had genotype 2 HCV infection (30 men and 25 women; mean age, 50.0 ± 11.6 years). All the patients with genotype 2 HCV infection were treated daily with IFN α-2b at 6 MU for two weeks, followed by treatment three times a week with IFN α-2b 6 MU for 22 weeks in combination with ribavirin. Ribavirin was given orally twice a day at a total daily dose of 600 mg for 24 weeks for patients who weighed 60 kg or less and 800 mg for patients who weighed more than 60 kg. Fifty of the 55 patients with genotype 2 HCV infection with available clinical data were retrospectively analyzed.

HCV markers

HCV genotype was determined by a direct sequencing of the amplified products generated during the Amplicor Monitor test (Roche Diagnostics, Branchburg, NJ)[25] with an ABI 3700 DNA sequencer (Perkin Elmer, Applied Biosystems, Foster City, CA).[26] HCV-RNA level was determined using Amplicor-M version 2 (Chugai-Roche Diagnostics, Tokyo, Japan).

Polymerase chain reaction (PCR) and determination of sequences of ISDR

Complementary DNA (cDNA) was prepared by reverse transcription using an RNA–PCR kit (Takara Bio, Shiga, Japan). In brief, 1 μL of RNA solution, extracted from 100 μL of serum and dissolved in 25 μL of RNase-free distilled water, was mixed with 4 μL of 1.5 mM $MgCl_2$ solution, 2 μL of 10× RNA–PCR buffer (100 mM Tris-HCl [pH 8.3], 500 mM KCl), 8.5 μL of RNase-free distilled H_2O, 2 μL of a dNTP mixture (10 mM dATP, dCTP, dGTP, dTTP), 1 μL of random 9-mers (5′-NNNNNNNNN-3′), 0.5 μL of RNase inhibitor (Takara Bio, Shiga, Japan) and 1 μL of reverse transcriptase (Takara Bio, Shiga, Japan), was reverse transcribed at 42°C for 30 min.

The first round PCR was performed using the external primers (sense primer; nt 6824–6846; 5′-TCTCAG CTCCCTTGCGATCCTGA-3′ and antisense primer; nt 7155–7139; 5′-GATGGTATCGAAGGCTC-3′) and 2.5 U of Ex Taq polymerase (Takara Bio, Shiga, Japan) with proofreading activity. The amplification conditions consisted of 94°C for 16 min followed by 40 cycles of 94°C for 1 min, 50°C for one minute and 72°C for one minute. One microliter of the first PCR product was used for the second PCR with internal primers (sense primer; nt 6950–6968; 5′-AGCTCCTCA GCGAGC CAGCT-3′, and antisense primer; nt 7104–7085; 5′-GATGGTATCGAAGGCTC-3′) and 0.5 μL of amplitaq gold (Roche Diagnostics, Branchburg, NJ). The amplification conditions of the second PCR were the same as those of the first PCR. The second PCR products were analyzed by 2% agarose gel electrophoresis, stained with ethidium bromide and visualized by UV transillumination.

Amplification products were purified on Wizard PCR Preps DNA purification resin (Promega, Madison, WI) and sequenced bidirectionally with the Dye Terminator Cycle Sequencing Ready Reaction kit (Perkin Elmer, Applied Biosystems, Foster City, CA) using the above PCR primers. Sequencing was performed using an automated DNA sequencer ABI 377 (Perkin Elmer, Applied Biosystems, Foster City, CA).

Histopathology

A liver biopsy was performed on each patient within six months before the start of therapy. The histopathological findings were assessed by grading inflammatory activity and the staging of fibrosis using the classification of Desmet *et al.*[27] by an experienced pathologist who had no knowledge of the clinical data of the patients.

Statistical analysis

The collected data were analyzed using the SPSS program, version 11.0J (SPSS, Chicago, IL). The distributions of continuous variables were analyzed using the

Table 1 Clinical background of patients

	Genotype of HCV			Difference
	2 ($n = 50$)	2a ($n = 32$)	2b ($n = 18$)	P (2a vs. 2b)
Age (years)	49.2 ± 11.8	50.6 ± 10.1	46.6 ± 12.2	0.25
Male	30 (60%)	20 (63%)	10 (56%)	0.63
Viral load (KIU/mL)	491.6 ± 286.2	420.3 ± 264.8	618.2 ± 279.0	0.02
Histopathology				
Grade (0/1/2/3)	0/29/17/2	0/16/13/1	0/13/4/1	0.34
Stage (0/1/2/3/4)	1/23/14/9/1	1/10/10/8/1	0/13/4/1/0	0.02
SVR	41 (82%)	27 (84%)	14 (78%)	0.15

SVR, sustained virological response.

Mann–Whitney *U*-test. Differences in proportions were tested using Fisher's exact test. Independent factors that may influence the response to combination therapy were identified using stepwise multiple logistic regression analysis. Variables with $P < 0.1$ at univariate analysis were retained for the multivariate logistic regression analysis. The significance of correlation was evaluated by Spearman's rank analysis. A two-tailed P-value of <0.05 was considered to indicate statistical significance.

RESULTS

Baseline characteristics of treated patients

TABLE 1 SHOWS the clinical background of the treated patients with genotype 2 HCV infection. The patients comprised 30 men and 20 women with a mean age of 49.2 ± 11.8 years. The patients with genotype 2a have lower viral loads and more severe fibrosis than those with genotype 2b HCV infection. The rate of SVR was 84% (27 of 32) in the patients with genotype 2a and 78% (14 of 18) in those with genotype 2b.

Amino acid sequence of ISDR

The amino acid sequence of ISDR was determined in 29 of the 32 patients with genotype 2a and 17 of the 18 patients with genotype 2b. The number of amino acid substitutions in ISDR was positively correlated with viral load (Spearman's rank correlation coefficient $r = -0.53$, $P < 0.001$). Figure 1 shows the amino acid sequences of ISDR. The prototype sequences of genotype 2a (D10749)[28] and 2b (D10988)[29] were determined to be the reference sequence for genotype 2a and 2b, respectively. The rate of SVR in the patients with no amino acid substitutions (wild type) in their ISDR sequence was 57% (8/14). In the patients with one to three amino acid substitutions (intermediate) and four or more substitutions (mutant) in their ISDR sequences, the rates of SVR were 85% (22/26) and 100% (8/8), respectively. In the patients with genotype 2a HCV infection, the rates of SVR in the wild, intermediate and mutant type ISDR were 63% (5/8), 80% (12/15) and 100% (8/8), respectively. In genotype 2b HCV infection, the rate of SVR in wild and intermediate type ISDR was 50% (3/6) and 91% (10/11), respectively.

Predictors of response

The characteristics of patients with SVR and those without were compared (Table 2). By univariate analysis, time of viral clearance from blood ($P = 0.018$) and

Table 2 Univariate logistic regression analysis for factors responsible for sustained virological response

	SVR	non-SVR	Univariate analysis P	Odds ratio
Age	51 (22–68)	52 (28–63)	0.805	0.992
Gender	21:17	7:2	0.195	0.329
Genotype (2a vs. 2b)	25:13	5:4	0.561	1.636
Histology of liver				
Grading (0/1/2/3)	0/21/16/2	0/8/1/0	0.086	6.438
Staging (0/1/2/3/4)	1/18/12/7/1	0/5/2/2/0	0.897	1.058
Pretreatment viral load (KIU/mL)	430 (8.7–>850)	710 (480–>850)	0.323	0.999
Time of viral clearance from blood (days)	14 (7–70)	52 (28–63)	0.018	0.649
Number of substituted amino acids in ISDR	1 (0–1)	0 (0–2)	0.048	3.716

SVR, sustained virological response.

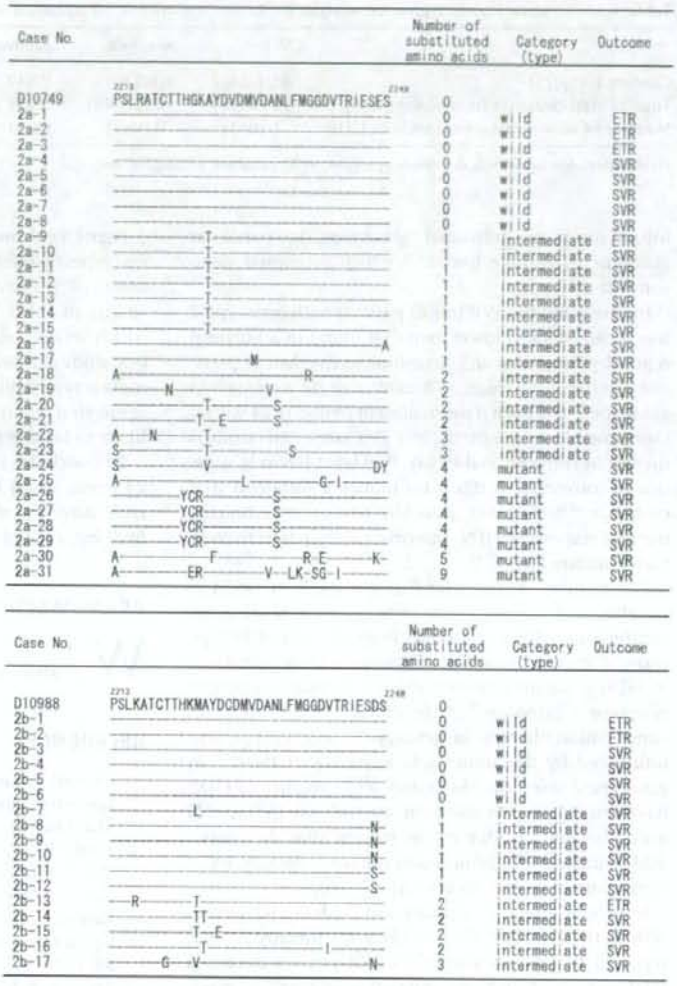

Case No.		Number of substituted amino acids	Category (type)	Outcome
	2218 2248			
D10749	PSLRATCTTHGKAYDVDMVDANLFMGGDVTRIESES	0		
2a-1		0	wild	ETR
2a-2		0	wild	ETR
2a-3		0	wild	ETR
2a-4		0	wild	SVR
2a-5		0	wild	SVR
2a-6		0	wild	SVR
2a-7		0	wild	SVR
2a-8		0	wild	SVR
2a-9	T	1	intermediate	ETR
2a-10	T	1	intermediate	SVR
2a-11	T	1	intermediate	SVR
2a-12	T	1	intermediate	SVR
2a-13	T	1	intermediate	SVR
2a-14	T	1	intermediate	SVR
2a-15	T	1	intermediate	SVR
2a-16	A	1	intermediate	SVR
2a-17	M	1	intermediate	SVR
2a-18	A R	2	intermediate	SVR
2a-19	N V	2	intermediate	SVR
2a-20	T S	2	intermediate	SVR
2a-21	T E S	2	intermediate	SVR
2a-22	A N T	3	intermediate	SVR
2a-23	S T S	3	intermediate	SVR
2a-24	S V DY	4	mutant	SVR
2a-25	A L G-I	4	mutant	SVR
2a-26	YCR S	4	mutant	SVR
2a-27	YCR S	4	mutant	SVR
2a-28	YCR S	4	mutant	SVR
2a-29	YCR S	4	mutant	SVR
2a-30	A F R E K-	5	mutant	SVR
2a-31	A ER V LK-SG-I	9	mutant	SVR

Case No.		Number of substituted amino acids	Category (type)	Outcome
	2213 2248			
D10988	PSLKATCTTHKMAYDCDMVDANLFMGGDVTRIESDS	0		
2b-1		0	wild	ETR
2b-2		0	wild	ETR
2b-3		0	wild	SVR
2b-4		0	wild	SVR
2b-5		0	wild	SVR
2b-6		0	wild	SVR
2b-7	L	1	intermediate	SVR
2b-8	N-	1	intermediate	SVR
2b-9	N-	1	intermediate	SVR
2b-10	N-	1	intermediate	SVR
2b-11	S-	1	intermediate	SVR
2b-12	S-	1	intermediate	SVR
2b-13	R T	2	intermediate	ETR
2b-14	TT	2	intermediate	SVR
2b-15	T E	2	intermediate	SVR
2b-16	T I	2	intermediate	SVR
2b-17	G V N-	3	intermediate	SVR

Figure 1 Figures 1a and 1b show patients with genotypes 2a and 2b, respectively. The rate of sustained virological response (SVR) in patients with no amino acid substitutions in interferon sensitivity determining region (ISDR) sequence (wild type) was 57% (8/14). In patients with one to three amino acid substitutions (intermediate) and four or more substitutions (mutant) in the ISDR sequences, the rates of SVR were 85% (22/26) and 100% (8/8), respectively. ETR, end of treatment for virological response.

amino acid mutations in the ISDR ($P = 0.048$) were found to be significantly linked to SVR. Because these variables were mutually correlated, multivariate analysis including histological grading was performed. In the final step, amino acid mutations in the ISDR (odds ratio [OR], 4.280; 95% confidence interval [CI], 1.139–16.038; $P = 0.031$) entered the model and could not be removed (Table 3). Therefore, amino acid mutations in ISDR are the only factor associated with SVR.

DISCUSSION

IN JAPAN, THE combination therapy of IFN and ribavirin for 24 weeks was approved in late 2001. It was shown that approximately 20% of patients infected with genotype 1b HCV with a high viral load attained SVR with this regimen.[30] Compared to those with genotype 1, patients with genotype 2 or 3 HCV infection are expected to achieve higher SVR rates.[12–14] However,

Table 3 Multivariate logistic regression analysis for factors responsible for sustained virological response

	SVR	non-SVR	Multivariate analysis *P*	Odds ratio
Grading (0/1/2/3)	0/21/16/2	0/8/1/0	0.547	2.141 (0180–25.463)
Time of viral clearance from blood (days)	14 (7–70)	52 (28–63)	0.091	0.552 (0.277–1.100)
Number of substituted amino acids in ISDR	1 (0–1)	0 (0–2)	0.031	4.280 (1.139–16.038)

ISDR, interferon sensitivity determining region; SVR, sustained virological response.

information on individual genotypes, in particular genotype 2, is quite limited,[31] which prompted us to conduct this study.

In this study the SVR rate of patients with genotype 2 was 82%, which is lower than that found in a previous report by Zeuzem *et al.*[31] According to the data of previous studies,[32,33] a high SVR rate may be expected in genotype 2 or 3 even if the treatment period is 24 weeks. One possible reason for the low SVR rate in this study is the use of conventional IFN-α. Pegylated IFN-α is superior to conventional IFN-α for inducing sustained viral clearance.[33,34] Another possible reason is ethnicity, because response to IFN–ribavirin combination therapy varies among races.[35,36]

The number of mutations in the ISDR of NS5A is variable and influences the efficacy of IFN–ribavirin combination therapy. Studies from Japan and Europe showed that the number of amino acid substitutions in ISDR influences the efficacy of IFN monotherapy in genotype 1 infection.[16–20] The efficacy of IFN–ribavirin combination therapy in genotype 1 infection is also influenced by the amino acid sequence of ISDR.[37] In genotype 2 infection, the amino acid sequence of ISDR has been reported to also correlate with the SVR to IFN monotherapy.[22–24] Our results suggest that the amino acid sequence of ISDR may also influence the efficacy of combination therapy in genotype 2 infection.

It is interesting that mutations in ISDR confer susceptibility to IFN–ribavirin combination therapy. It was reported that NS5A suppresses PKR protein kinase, a mediator of IFN-induced antiviral resistance[38] in genotype 1 infection. Multiple ISDR mutations probably abrogate this action of NS5A to inhibit PKR.[39] However, whether the mechanisms are also applicable to genotype 2 infection is still unclear and needs clarification.

Our study showed that about 20% of the patients with genotype 2 HCV infection were not cured by the combination therapy for 24 weeks. However, all of the uncured patients were relapsers, whose viral loads were cleared from the serum at the end of treatment. Therefore, it can be expected that these patients may be cured by a longer treatment, which should be studied further.

Figure 1a showed that cases 26, 27, 28 and 29, with no common infectious source, had the same mutations. Most of previous reported cases with mutant-type strains of ISDR had different amino acid sequences, which seems contradictory to our results.[22–24] However, one study showed that two of the four cases shared one mutant type sequence of ISDR.[23] These results imply that some viral strains with mutant type ISDR sequence are likely to be selected, which await further study.

To conclude, IFN–ribavirin combination therapy for 24 weeks cured 80% of the patients with genotype 2 HCV. Amino acid mutations in ISDR may determine the final outcome of the combination therapy.

ACKNOWLEDGMENTS

WE THANK MS Mie Kanke for her excellent technical assistance.

REFERENCES

1 Tong MJ, el-Farra NS, Reikes AR, Co RL. Clinical outcomes after transfusion-associated hepatitis C. *N Engl J Med* 1995; **332**: 1463–6.
2 Takahashi M, Yamada G, Miyamoto R, Doi T, Endo H, Tsuji T. Natural course of chronic hepatitis C. *Am J Gastroenterol* 1993; **88**: 240–3.
3 Yano M, Kumada H, Kage M *et al.* The long-term pathological evolution of chronic hepatitis C. *Hepatology* 1996; **23**: 1334–40.
4 Kiyosawa K, Umemura T, Ichijo T *et al.* Hepatocellular carcinoma: recent trends in Japan. *Gastroenterology* 2004; **127**: S17–26.
5 Iino S. Natural history of hepatitis B and C virus infections. *Oncology* 2002; **62** (Suppl 1): 18–23.
6 Hu KQ, Tong MJ. The long-term outcomes of patients with compensated hepatitis C virus-related cirrhosis and history of parenteral exposure in the United States. *Hepatology* 1999; **29**: 1311–16.
7 Camma C, Giunta M, Pinzello G, Morabito A, Verderio P, Pagliaro L. Chronic hepatitis C and interferon alpha: conventional and cumulative meta-analyses of randomized controlled trials. *Am J Gastroenterol* 1999; **94**: 581–95.

8 Poynard T, Leroy V, Cohard M *et al.* Meta-analysis of interferon randomized trials in the treatment of viral hepatitis C: effects of dose and duration. *Hepatology* 1996; **24**: 778–89.
9 Niederau C, Heintges T, Haussinger D. Treatment of chronic hepatitis C with a-interferon: an analysis of the literature. *Hepatogastroenterology* 1996; **43**: 1544–56.
10 Lai MY, Kao JH, Yang PM *et al.* Long-term efficacy of ribavirin plus interferon alfa in the treatment of chronic hepatitis C. *Gastroenterology* 1996; **111**: 1307–12.
11 Reichard O, Norkrans G, Fryden A, Braconier JH, Sonnerborg A, Weiland O. Randomised, double-blind, placebo-controlled trial of interferon alpha-2b with and without ribavirin for chronic hepatitis C. The Swedish Study Group. *Lancet* 1998; **351**: 83–7.
12 Poynard T, Marcellin P, Lee SS *et al.* Randomised trial of interferon alpha2b plus ribavirin for 48 weeks or for 24 weeks versus interferon alpha2b plus placebo for 48 weeks for treatment of chronic infection with hepatitis C virus. International Hepatitis Interventional Therapy Group (IHIT). *Lancet* 1998; **352**: 1426–32.
13 McHutchison JG, Gordon SC, Schiff ER *et al.* Interferon alfa-2b alone or in combination with ribavirin as initial treatment for chronic hepatitis C. Hepatitis Interventional Therapy Group. *N Engl J Med* 1998; **339**: 1485–92.
14 Davis GL, Esteban-Mur R, Rustgi V *et al.* Interferon alfa-2b alone or in combination with ribavirin for the treatment of relapse of chronic hepatitis C. International Hepatitis Interventional Therapy Group. *N Engl J Med* 1998; **339**: 1493–9.
15 Zeuzem S. Heterogeneous virologic response rates to interferon-based therapy in patients with chronic hepatitis C: who responds less well? *Ann Intern Med* 2004; **140**: 370–81.
16 Enomoto N, Sakuma I, Asahina Y *et al.* Mutations in the nonstructural protein 5A gene and response to interferon in patients with chronic hepatitis C virus 1b infection. *N Engl J Med* 1996; **334**: 77–81.
17 Kurosaki M, Enomoto N, Murakami T *et al.* Analysis of genotypes and amino acid residues 2209–2248 of the NS5A region of hepatitis C virus in relation to the response to interferon-beta therapy. *Hepatology* 1997; **25**: 750–3.
18 Saiz JC, Lopez-Labrador FX, Ampurdanes S *et al.* The prognostic relevance of the nonstructural 5A gene interferon sensitivity determining region is different in infections with genotype 1b and 3a isolates of hepatitis C virus. *J Infect Dis* 1998; **177**: 839–47.
19 Chayama K, Tsubota A, Kobayashi M *et al.* Pretreatment virus load and multiple amino acid substitutions in the interferon sensitivity-determining region predict the outcome of interferon treatment in patients with chronic genotype 1b hepatitis C virus infection. *Hepatology* 1997; **25**: 745–9.
20 Yoshioka K, Kobayashi M, Orito E *et al.* Biochemical response to interferon therapy correlates with interferon sensitivity-determining region in hepatitis C virus genotype 1b infection. *J Viral Hepat* 2001; **8**: 421–9.
21 Schinkel J, Spaan WJ, Kroes AC. Meta-analysis of mutations in the NS5A gene and hepatitis C virus resistance to interferon therapy: uniting discordant conclusions. *Antivir Ther* 2004; **9**: 275–86.
22 Murakami T, Enomoto N, Kurosaki M, Izumi N, Marumo F, Sato C. Mutations in nonstructural protein 5A gene and response to interferon in hepatitis C virus genotype 2 infection. *Hepatology* 1999; **30**: 1045–53.
23 Kobayashi M, Watanabe K, Ishigami M *et al.* Amino acid substitutions in the nonstructural region 5A of hepatitis C virus genotypes 2a and 2b and its relation to viral load and response to interferon. *Am J Gastroenterol* 2002; **97**: 988–98.
24 Akuta N, Suzuki F, Tsubota A *et al.* Association of amino acid substitution pattern in nonstructural protein 5A of hepatitis C virus genotype 2a low viral load and response to interferon monotherapy. *J Med Virol* 2003; **69**: 376–83.
25 Lee SC, Antony A, Lee N *et al.* Improved version 2.0 qualitative and quantitative AMPLICOR reverse transcription-PCR tests for hepatitis C virus RNA: calibration to international units, enhanced genotype reactivity, and performance characteristics. *J Clin Microbiol* 2000; **38**: 4171–9.
26 Mukaide M, Tanaka Y, Kakuda H *et al.* New combination test for hepatitis C virus genotype and viral load determination using Amplicor GT HCV MONITOR test v2.0. *World J Gastroenterol* 2005; **11**: 469–75.
27 Desmet VJ, Gerber M, Hoofnagle JH, Manns M, Scheuer PJ. Classification of chronic hepatitis: diagnosis, grading and staging. *Hepatology* 1994; **19**: 1513–20.
28 Okamoto H, Okada S, Sugiyama Y *et al.* Nucleotide sequence of the genomic RNA of hepatitis C virus isolated from a human carrier: comparison with reported isolates for conserved and divergent regions. *J Gen Virol* 1991; **72**: 2697–704.
29 Okamoto H, Kurai K, Okada S *et al.* Full-length sequence of a hepatitis C virus genome having poor homology to reported isolates: comparative study of four distinct genotypes. *Virology* 1992; **188**: 331–41.
30 Tsubota A, Arase Y, Suzuki F *et al.* High-dose interferon alpha-2b induction therapy in combination with ribavirin for Japanese patients infected with hepatitis C virus genotype 1b with a high baseline viral load. *J Gastroenterol* 2004; **39**: 155–61.
31 Zeuzem S, Hultcrantz R, Bourliere M *et al.* Peginterferon alfa-2b plus ribavirin for treatment of chronic hepatitis C in previously untreated patients infected with HCV genotypes 2 or 3. *J Hepatol* 2004; **40**: 993–9.
32 Cornberg M, Huppe D, Wiegand J *et al.* Treatment of chronic hepatitis C with PEG-interferon alpha-2b and ribavirin: 24 weeks of therapy are sufficient for HCV genotype 2 and 3. *Z Gastroenterol* 2003; **41**: 517–22.
33 Manns MP, McHutchison JG, Gordon SC *et al.* Peginterferon alfa-2b plus ribavirin compared with interferon

alfa-2b plus ribavirin for initial treatment of chronic hepatitis C: a randomised trial. *Lancet* 2001; **358**: 958–65.
34 Lee SD, Yu ML, Cheng PN *et al.* Comparison of a 6-month course peginterferon alpha-2b plus ribavirin and interferon alpha-2b plus ribavirin in treating Chinese patients with chronic hepatitis C in Taiwan. *J Viral Hepat* 2005; **12**: 283–91.
35 McHutchison JG, Poynard T, Pianko S *et al.* The impact of interferon plus ribavirin on response to therapy in black patients with chronic hepatitis C. The International Hepatitis Interventional Therapy Group. *Gastroenterology* 2000; **119**: 1317–23.
36 Hepburn MJ, Hepburn LM, Cantu NS, Lapeer MG, Lawitz EJ. Differences in treatment outcome for hepatitis C among ethnic groups. *Am J Med* 2004; **117**: 163–8.
37 Hung CH, Lee CM, Lu SN *et al.* Mutations in the NS5A and E2-PePHD region of hepatitis C virus type 1b and correlation with the response to combination therapy with interferon and ribavirin. *J Viral Hepat* 2003; **10**: 87–94.
38 Gale MJ Jr, Korth MJ, Tang NM *et al.* Evidence that hepatitis C virus resistance to interferon is mediated through repression of the PKR protein kinase by the nonstructural 5A protein. *Virology* 1997; **230**: 217–27.
39 Noguchi T, Satoh S, Noshi T *et al.* Effects of mutation in hepatitis C virus nonstructural protein 5A on interferon resistance mediated by inhibition of PKR kinase activity in mammalian cells. *Microbiol Immunol* 2001; **45**: 829–40.

Int. J. Cancer: **122,** 124–131 (2008)

Hepatitis C virus core protein induces spontaneous and persistent activation of peroxisome proliferator-activated receptor α in transgenic mice: Implications for HCV-associated hepatocarcinogenesis

Naoki Tanaka[1,2]*, Kyoji Moriya[3], Kendo Kiyosawa[2], Kazuhiko Koike[3] and Toshifumi Aoyama[1]

[1]*Department of Metabolic Regulation, Institute on Aging and Adaptation, Shinshu University Graduate School of Medicine, Matsumoto, Japan*

[2]*Division of Gastroenterology, Department of Internal Medicine, Shinshu University School of Medicine, Matsumoto, Japan*

[3]*Department of Internal Medicine, Graduate School of Medicine, University of Tokyo, Tokyo, Japan*

Persistent infection of hepatitis C virus (HCV) can lead to a high risk for hepatocellular carcinoma (HCC). HCV core protein plays important roles in HCV-related hepatocarcinogenesis, because mice carrying the core protein exhibit multicentric HCCs without hepatic inflammation and fibrosis. However, the precise mechanism of hepatocarcinogenesis in these transgenic mice remains unclear. To evaluate whether the core protein modulates hepatocyte proliferation and apoptosis *in vivo*, we examined these parameters in 9- and 22-month-old transgenic mice. Although the numbers of apoptotic hepatocytes and hepatic caspase 3 activities were similar between transgenic and nontransgenic mice, the numbers of proliferating hepatocytes and the levels of numerous proteins such as cyclin D1, cyclin-dependent kinase 4 and c-Myc, were markedly increased in an age-dependent manner in the transgenic mice. This increase was correlated with the activation of peroxisome proliferator-activated receptor α (PPARα). In these transgenic mice, spontaneous and persistent PPARα activation occurred heterogeneously, which was different from that observed in mice treated with clofibrate, a potent peroxisome proliferator. We further demonstrated that stabilization of PPARα through a possible interaction with HCV core protein and an increase in nonesterified fatty acids, which may serve as endogenous PPARα ligands, in hepatocyte nuclei contributed to the core protein-specific PPARα activation. In conclusion, these results offer the first suggestion that HCV core protein induces spontaneous, persistent, age-dependent and heterogeneous activation of PPARα in transgenic mice, which may contribute to the age-dependent and multicentric hepatocarcinogenesis mediated by the core protein.

Key words: cell-cycle regulator; peroxisome; nuclear stabilization; heterogeneous PPARα activation

Hepatitis C virus (HCV) is one of the major causes of chronic hepatitis, and persistent infection with this virus can lead to a high incidence of hepatocellular carcinoma (HCC).[1,2] The prevalence of HCC because of chronic HCV infection has increased over the past two decades,[3,4] and chronic HCV infection has therefore been recognized as a serious disease. However, the precise mechanism of hepatocarcinogenesis during chronic HCV infection remains unclear.

Many experiments using cell culture systems have suggested the possibility that HCV core protein itself can modulate various cellular functions and can be directly linked to the development of HCV-related HCC.[5] For example, HCV core protein transforms rat embryo fibroblasts to a tumorigenic phenotype in cooperation with the H-*ras* oncogene,[6] suppresses *c-myc*-related apoptosis[7] and transcription of the *p53* gene,[8] interacts with a variety of proteins, including helicase, lymphotoxin-β receptor, or dead box protein, and modulates their functions.[9] We further established transgenic mouse lines carrying the HCV core gene, in which the core protein is constitutively expressed in the liver at levels similar to that found in chronic hepatitis C patients.[10] These mice exhibited multicentric hepatic adenomas, and developed HCCs in an age-dependent manner.[11] The livers of these mice were almost free of inflammation, necrosis and fibrosis,[10,11] suggesting that the core protein itself has a hepatocarcinogenic potential *in vivo*. However, the molecular mechanism of the development of HCC in the transgenic mice has not been fully understood.

In the livers of HCV core gene transgenic mice, an age-dependent increase in oxidative stress and resultant DNA damage were found,[12] and these effects may contribute to or facilitate the development of HCC. Another possible mechanism of hepatocarcinogenesis is continuous enhancement of hepatocyte proliferation. Cell proliferation and apoptosis are highly regulated processes for maintaining homeostasis in many organs, and during the carcinogenic process, sustained imbalance generally precedes cancer.[13,14] For example, in patients with chronic HCV infection, high hepatocyte proliferative activity relative to apoptosis may reliably predict a new development of HCC.[15] However, there is no information about whether or not hepatocyte proliferation accelerates persistently in mice carrying the HCV core gene, and no information about how the core protein promotes hepatocyte proliferation *in vivo*. In the current study, we began to examine changes in the parameters of hepatocyte proliferation and apoptosis in the transgenic mice.

Material and methods

Animals and treatments

HCV core gene transgenic mice on a C57BL/6N genetic background were produced as described earlier.[10] Because HCC developed preferentially in male transgenic mice,[11] 9- and 22-month-old male mice ($n = 8$ for either age group) were adopted. Sex- and age-matched nontransgenic mice ($n = 8$ for either age group) were used as controls. These mice were fed an ordinary diet and were treated in a specific pathogen-free state according to the institutional guidelines. For additional experiment, male wild-type mice fed a control diet containing 0.5% clofibrate for 2 weeks ($n = 8$) were used. All mice were killed by cervical dislocation and the livers were excised. When a hepatic tumor was present, it was removed and the remaining liver tissue was used. All experiments were performed in accordance with animal study protocols approved by the Shinshu University School of Medicine.

Abbreviations: AOX, acyl-CoA oxidase; CDK, cyclin-dependent kinase; DAB, 3,3'-diaminobenzidine; FITC, fluorescein isothiocyanate; HCC, hepatocellular carcinoma; HCV, hepatitis C virus; L-FABP, liver-type fatty acid-binding protein; NEFA, nonesterified fatty acid; PBS, phosphate-buffered saline; PCNA, proliferating cell nuclear antigen; PMSF, phenylmethylsulfonyl fluoride; PPAR, peroxisome proliferator-activated receptor; PT, peroxisomal thiolase; RXR, retinoid X receptor; SDS, sodium dodecyl sulfate; TUNEL, terminal deoxynucleotidyl transferase-mediated deoxyuridine triphosphate nick-end labeling.

***Correspondence to:** Department of Metabolic Regulation, Institute on Aging and Adaptation, Shinshu University Graduate School of Medicine, 3-1-1 Asahi, Matsumoto, 390-8621, Japan. Fax: +81-26-337-3094. E-mail: naopi@hsp.md.shinshu-u.ac.jp

Received 2 May 2007; Accepted after revision 28 June 2007
DOI 10.1002/ijc.23056
Published online 31 August 2007 in Wiley InterScience (www.interscience.wiley.com).

Preparation of hepatocyte nuclear fraction

Approximately 200 mg of liver tissues was transferred to a chilled Dounce homogenizer (Wheaton, Milliville, NJ) and homogenized on ice by 30 strokes in 1.2 mL of nuclei buffer [300 mM sucrose in 10 mM Tris-HCl, pH 7.4, 15 mM NaCl, 5 mM $MgCl_2$ and 0.25 mM phenylmethylsulfonyl fluoride (PMSF)]. The homogenate was filtered through gauze and centrifuged at 4,500*g* for 5 min at 4°C. The resulting pellet was resuspended, layered over 2 mL of nuclei buffer containing 2 M sucrose, and centrifuged at 23,000*g* for 1 hr at 4°C. The pellet obtained after ultracentrifugation was resuspended in 250 μL of nuclei buffer and used as the nuclear fraction. Preparation of nuclear fraction from isolated hepatocytes was performed as described elsewhere.[16]

Immunoblot analysis

Protein concentration was measured colorimetrically by a BCA™ Protein Assay kit (Pierce, Rockford, IL). For analysis of fatty acid-metabolizing enzymes and protein, whole liver lysate (10–20 μg protein) was subjected to 10% sodium dodecyl sulfate (SDS)-polyacrylamide gel electrophoresis.[17] For analysis of other proteins, hepatocyte nuclear fraction (100 μg protein) or whole liver lysate (200–300 μg protein) was subjected to electrophoresis. After electrophoresis, the proteins were transferred to nitrocellulose membranes, which were incubated with the primary antibody, followed by alkaline phosphatase-conjugated goat anti-rabbit or anti-mouse IgG. The origin of the primary rabbit polyclonal antibodies against fatty acid-metabolizing enzymes and protein was described earlier.[17] For immunoblot analysis of peroxisome proliferator-activated receptor α (PPARα), a polyclonal anti-mouse antibody[18] or commercial antibody (Santa Cruz Biotechnology, Santa Cruz, CA) was used. The antibodies against cell-cycle regulators and oncogene products were purchased commercially (Santa Cruz Biotech.).[19] Equal loading of the protein obtained from whole liver lysate and nuclear fraction was confirmed by reprobing the membranes with an antibody against β-actin and histone H1, respectively. The band intensity of nuclear PPARα was quantified densitometrically, normalized to that of histone H1, and subsequently expressed as the fold changes relative to that of 9-month-old nontransgenic mice.

mRNA analysis

Total liver RNA was extracted with an RNeasy Mini Kit™ (Qiagen, Valencia, CA). Five microgram of RNA was electrophoresed on 1.1 M formaldehyde-containing 1% agarose gels and transferred to nylon membranes by capillary blotting in 20× SSC buffer (3 M NaCl and 300 mM sodium citrate, pH 7.0) overnight. The membranes were hybridized with ^{32}P-labeled cDNA probes. The blots were exposed to a phosphorimager screen cassette and were analyzed using a Molecular Dynamics Storm 860 Phosphorimager system (Sunnyvale, CA). The origin of the cDNA probes has been described elsewhere.[17–19] Northern blot of β-actin was used as the internal control. The blot intensity was quantified, normalized to that of β-actin and subsequently expressed as the fold changes relative to that of 9-month-old nontransgenic mice.

Pulse-label and pulse-chase experiment

Parenchymal hepatocytes were isolated from transgenic and control mice by the modified *in situ* perfusion method.[20] After perfusion with 0.05% collagenase solution (Wako, Osaka, Japan), the isolated hepatocytes were washed thrice by means of differential centrifugation and the dead cells removed by density gradient centrifugation on Percoll (Amersham Pharmacia Biotech, Buckinghamshire, UK). The live hepatocytes were washed and suspended in William's E medium containing 5% fetal bovine serum. When the viability of the isolated hepatocytes exceeded 85% as determined by the trypan blue exclusion test, the following experiments were conducted. The isolated hepatocytes were washed twice and incubated in methionine-free medium containing 5% dialyzed fetal bovine serum for 1 hr at 37°C. The medium was replaced with the same medium containing 300 μCi/mL of [^{35}S]methionine (Amersham Pharmacia Biotech.). After 3-hr of incubation, the labeled medium was changed to the standard medium and the preparation was chased for 4, 8 or 16 hr. The labeled cells were washed, homogenized and centrifuged for preparation of the nuclear fraction. The levels of radioactivity in the homogenates of the pulse-labeled preparations were similar between the transgenic and the nontransgenic mice, suggesting that the [^{35}S]methionine uptake capacity in the former hepatocytes is similar to that in the latter. The nuclear fraction was lysed in RIPA buffer [10 mM Tris-HCl, pH 7.4, 0.2% sodium deoxycholate, 0.2% Nonidet P-40, 0.1% SDS, 0.25 mM PMSF, 10 μg/mL aprotinin]. The lysate was incubated for 3 hr at 4°C with purified anti-PPARα antibody. The immune complexes were precipitated with *Staphylococcus aureus* protein A bound to agarose beads. After the precipitates had been washed in RIPA buffer, the labeled proteins were resolved by 10% SDS-polyacrylamide gel electrophoresis and visualized by autoradiography. The nuclear fractions of the pulse-labeled preparations were also used for immunoblot analysis of PPARα.

Affinity chromatography for PPARα complex

All procedures were performed at 4°C. The nuclear fraction from the mouse liver was mixed with a 4-fold volume of a solution containing 12.5 mM potassium phosphate, pH 7.5, 25 mM NaCl, 0.25% Tween 20 and 0.1 mM PMSF. The mixture was briefly sonicated with a microsonicator, the Powersonic Model 50 (Yamato, Tokyo, Japan), and then centrifuged at 100,000*g* for 20 min. The supernatant was applied to an immobilized anti-PPARα IgG column (1.0 × 4.0 cm^2), prepared with the Affigel HZ Immunoaffinity kit^R (Bio-Rad, Hercules, CA) and equilibrated with 10 mM potassium phosphate, pH 7.5, 20 mM NaCl and 0.2% Tween 20. The solution was again passed through the column and this was repeated at least thrice. The column was washed and the elution performed with 150 mM sodium citrate, pH 3.0, and 200 mM NaCl, in a total volume of 2 mL. The eluate was resolved by 10 and 15% SDS-polyacrylamide gel electrophoresis for PPARα and the HCV core protein, respectively. The core protein expressed in COS cells was used as a positive marker.[21] The monoclonal antibody against the core protein was purchased commercially (ViroGen, Watertown, MA).

Cytochemical staining of peroxisomes

Liver peroxisome proliferation was evaluated by using 3,3′-diaminobenzidine (DAB) staining for catalase according to the method of Novikoff and Goldfischer with minor modifications.[22] Small pieces of liver were fixed with 2% glutaraldehyde in 100 mM sodium cacodylate buffer, pH 7.2, for 3 hr at 4°C, rinsed with sodium cacodylate buffer and cut into 100-μm sections with a Lancer^R Vibratome 1000 (Lancer, Bridgeton, MO). These sections were then incubated for 1 hr at 37°C in the DAB reaction medium (0.2% DAB tetrahydrochloride in 50 mM propanediol, pH 9.7, 5 mM KCN, 0.05% H_2O_2) and postfixed with 1% OsO_4 in 100 mM sodium phosphate, pH 7.4 for 1 hr. The sections were dehydrated through a graded series of ethanol and acetone treatments and embedded in Epok 812 (Oken, Tokyo, Japan). One micrometer sections were prepared, counterstained with 0.1% toluidine blue solution and examined by light microscopy. For electron microscopic examination, 0.1-μm sections were cut with a diamond knife, collected on grid meshes, stained with lead citrate and uranyl acetate and visualized with a JEM 1200EX II electron microscope (JEOL, Tokyo, Japan) at an accelerating voltage of 80 keV.

Morphometry of hepatic peroxisomes

Morphometric analysis of DAB-stained peroxisomes was carried out using electron photomicrographs. For each mouse, 10 independent fields in the pericentral area of liver lobuli were photomicrographed at an original magnification of 4,000×. At this magnification, peroxisomes smaller than 450 nm were clearly

identified. Peroxisomes were easily detected because of their high contrast because of the positive DAB reaction. In each frame, the number of peroxisomal profiles and the area of each individual profile were determined. The numerical density and volume density of peroxisomes were calculated using the following equations: numerical density (number/μm^2) = $N_P/(A_T - A_{empty})$, and volume density (%) = $A_{TP}/(A_T - A_{empty}) \times 100$, where N_P is the peroxisome number in the test area, A_T is the test area, A_{empty} is the area of the vascular and biliary lumens and that of the hepatocyte nuclei and lipid droplets, and A_{TP} is the area of total peroxisomal profiles in the test area. The area was measured with a Luzex AP image analyzer (Nireco, Tokyo, Japan).

Immunofluorescence staining

Liver samples were fixed in 4% paraformaldehyde in phosphate-buffered saline (PBS), embedded in Tissue-Tek O.C.T compound™ (Sakura Finetek, Torrance, CA) and frozen. Frozen liver 5-μm sections were prepared, washed with PBS, blocked with bovine serum albumin for 1 hr and incubated overnight with rabbit polyclonal antibodies against cyclin D1 (1:50 dilution)[19] and PPARα (1:100 dilution),[18] and with mouse monoclonal antibody against proliferating cell nuclear antigen (PCNA) (1:100 dilution).[19] After 5 washes with PBS, these sections were incubated with fluorescein isothiocyanate (FITC)-conjugated goat anti-rabbit IgG (Jackson ImmunoResearch, West Grove, PA) or donkey anti-mouse IgG (Dako). The sections were mounted and viewed with an Olympus Fluoview confocal laser scanning microscope (Olympus, Tokyo, Japan). Two-thousand hepatocyte nuclei were examined for each mouse, and the number of hepatocyte nuclei stained with the antibodies against cyclin D1, PPARα and PCNA was counted and expressed as a percentage.

Assessment of apoptotic hepatocytes

Liver samples were cut into small pieces and then fixed in 4% paraformaldehyde in PBS. These samples were dehydrated, embedded in paraffin and cut into 4-μm sections. The terminal deoxynucleotidyl transferase-mediated deoxyuridine triphosphate nick-end labeling (TUNEL) assay was performed using a MEBSTAIN Apoptosis Kit II (Medical and Biological Laboratories, Nagoya, Japan). The number of apoptotic hepatocytes in 2,000 hepatocytes was counted for each mouse, and expressed as a percentage.

Other methods

Hepatic caspase 3 activity was measured as described elsewhere.[23] For analysis of the nuclear contents of nonesterified fatty acids (NEFAs), ~150 μL of the hepatocyte nuclear fraction, containing 1–2 mg of protein, was treated with a microsonicator. Lipid extraction was performed according to a modification of the method developed by Folch *et al.*[24] and the nuclear content of NEFAs was measured with a *NEFA* C-test kit™ (Wako).

Statistical analysis

Statistical analysis was performed by means of Student's *t*-test. The results are expressed as the mean ± standard deviation. A probability value of less than 0.05 was considered to be statistically significant.

Results

Accelerated hepatocyte proliferation in HCV core gene transgenic mice

To evaluate hepatocyte proliferative activity, PCNA-positive hepatocytes were counted in male transgenic mice and nontransgenic mice. Although hepatic inflammation and hepatocyte necrosis were not detected in either group, the numbers of PCNA-positive hepatocytes were significantly increased in the 9-month-old transgenic mice compared with the 9-month-old nontransgenic mice (Fig. 1*a*). The increase was more significant in the 22-month-old transgenic mice (Fig. 1*a*). The numbers of PCNA-positive hepatocytes in the 22-month-old transgenic mice corresponded with those in HCV polyprotein-expressing transgenic mice with HCC.[25] On the other hand, the parameters of apoptosis, *i.e.*, the numbers of TUNEL-positive hepatocytes and hepatic caspase 3 activity, remained unchanged between the 2 groups at the same ages (Figs. 1*b* and 1*c*). These results suggest that spontaneous hepatocyte proliferation occurs as early as the age of 9 months and persists for a long time in HCV core gene transgenic mice.

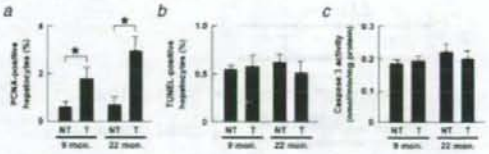

FIGURE 1 – Increase in hepatocyte proliferative activity. (*a*) The number of PCNA-positive hepatocytes. Two-thousand hepatocyte nuclei were examined for each mouse, and the number stained with anti-PCNA antibody was counted. Results are expressed as the mean ± standard deviation ($n = 8$). *, $p < 0.05$ between the transgenic mice and the nontransgenic mice; NT, nontransgenic mice; T, transgenic mice; 9 mon, 9-month-old mice; 22 mon, 22-month-old mice. (*b*) The number of apoptotic hepatocytes. The number of TUNEL-positive hepatocytes in 2,000 hepatocytes was determined for each mouse. Results are expressed as the mean ± standard deviation ($n = 8$). (*c*) Caspase 3 activity. Results are expressed as the mean ± standard deviation ($n = 8$).

Simultaneous induction of cell-cycle regulators and oncogene products in HCV core gene transgenic mouse livers

To examine the changes in the expression of proteins associated with hepatocyte division, the livers of the 9- and 22-month-old mice were subjected to immunoblot analysis. The levels of many proteins including cell-cycle regulators [cyclin-dependent kinase (CDK) 1, 2 and 4, cyclin D1 and E, and PCNA], and oncogene products (c-Myc, c-Fos and c-Ha-Ras) were significantly higher in the 22-month-old transgenic mice than in the control mice (Fig. 2). The levels of CDK inhibitors such as p16 and p21 were similar between the 2 groups. Similar results were obtained from the 9-month-old transgenic mice (data not shown). Time course changes in the expression of key G1-S checkpoint regulators, cyclin D1 and CDK4, are shown in Figure 3*a*. The simultaneous increase in the expression of cyclin D1 and CDK4 in the transgenic mice was continuous and more pronounced with age. Northern blot analysis revealed that the increase of these proteins occurred at the transcriptional level (Figs. 3*b* and 3*c*). Thus, these results reveal that various proteins which accelerate cell-cycle progression were induced simultaneously, persistently and age-dependently in the transgenic mice.

Correlative induction of PPARα targets in HCV core gene transgenic mouse livers

As shown in Figure 2, the expression of many kinds of cell-cycle regulators and oncogene products is known to be induced by the functional activation of PPARα.[19,26–30] To investigate whether PPARα is activated in the livers of transgenic mice, the expression of representative PPARα target genes,[30] acyl-CoA oxidase (AOX), peroxisomal thiolase (PT) and liver-type fatty acid-binding protein (L-FABP), was examined. As demonstrated in Figure 3*a*, the levels of AOX, PT, and L-FABP were increased in the 9-month-old transgenic mice compared with the nontransgenic mice, and the increase was more pronounced in the 22-month-old transgenic mice. Northern blot analysis demonstrated that the increase in these PPARα targets was based on the increase in the transcriptional activity (Figs. 3*b* and 3*c*). The increase in the

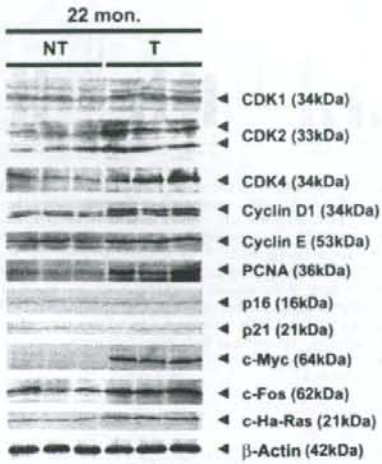

FIGURE 2 – Immunoblot analysis of cell-cycle regulators and oncogene products. Whole liver lysate (200 μg) was loaded in each lane. The band of β-actin was used as the loading control. The apparent molecular weight is indicated in parentheses. 22 mon, 22-month-old mice; NT, nontransgenic mice; T, transgenic mice.

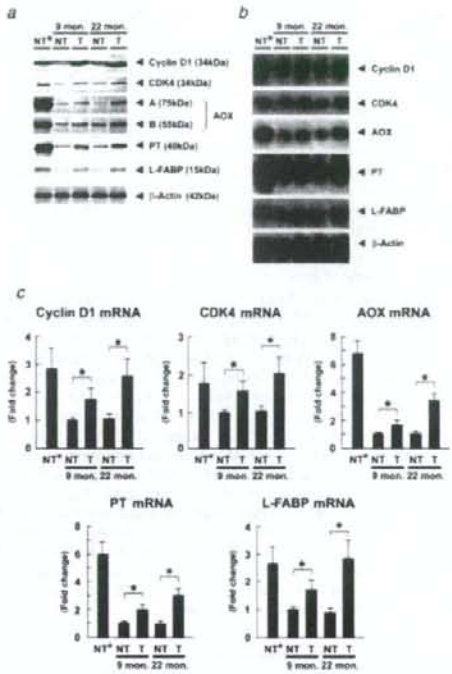

FIGURE 3 – Analysis of PPARα-regulated proteins. (*a*) Immunoblot analysis of cell-cycle regulators and fatty acid-metabolizing enzymes and proteins. Since no significant individual differences in the same mouse group were found in the preliminary experiments, 10 mg of liver pieces prepared from each mouse (n = 8/group) was mixed and homogenized. Whole liver lysate (200 μg for cyclin D1 and CDK4, and 20 μg for others) was loaded in each lane. The band of β-actin was used as the loading control. Results are representative of 4 independent experiments. The apparent molecular weight is indicated in parentheses. 9 mon, 9-month-old mice; 22 mon, 22-month-old mice; NT, nontransgenic mice; T, transgenic mice; NT*, nontransgenic mice treated with a control diet containing 0.5% clofibrate for 2 weeks; A and B, full-length and truncated AOX, respectively. (*b*) Northern blot analysis concerning the proteins in (*a*). Ten milligram of liver pieces from each mouse (n = 8/group) was mixed and homogenized, and total liver RNA was extracted. Hepatic RNA (5 μg) was separated on a denaturing gel, transferred to membranes and hybridized with the indicated ^{32}P-labeled cDNA probes. The blot of β-actin was used as the internal control. Results are representative of 4 independent experiments. (*c*) Quantification of hepatic mRNA levels. The mRNA level was quantified using a phosphorimager, normalized to that of β-actin, and subsequently normalized to that of 9-month-old nontransgenic mice. Results were obtained from 4 independent experiments and expressed as the mean ± standard deviation. Abbreviations are identical with those in (*b*). *, $p < 0.05$ between the transgenic mice and the nontransgenic mice.

mRNA expression of AOX, PT and L-FABP corresponded exactly with that of cyclin D1 or CDK4 (Figs. 3*b* and 3*c*). Therefore, these results demonstrate the strong correlation between continuous and age-dependent induction of cell-cycle regulators and functional activation of PPARα in these transgenic mice. Furthermore, the induction of these 5 proteins was also observed in wild-type mice treated with clofibrate, a potent PPARα activator; however, the degree of the induction of AOX and PT in the transgenic mice was smaller than that in the clofibrate-treated wild-type mice (Fig. 3), suggesting that the PPARα activation found in the transgenic mice was not as intense as that in the mice treated with clofibrate.

Histological evaluation of PPARα activation

An increase in the numbers of peroxisomes is associated with PPARα activation.[18] To determine whether peroxisome proliferation occurs in the HCV core gene transgenic mice, cytochemical staining for peroxisomal catalase was performed. A scattered distribution of hepatocytes with numerous peroxisomes was observed in the 9-month-old transgenic mice (Fig. 4*a*). Such hepatocytes were also found in the 22-month-old transgenic mouse livers (Fig. 4*a*). In contrast, almost all of the hepatocytes in the clofibrate-treated mice showed significant peroxisome proliferation (Fig. 4*a*). To quantitatively evaluate the degree of peroxisome proliferation, morphometric analysis of peroxisomes was conducted. The numerical density and volume density were significantly increased in the transgenic mice compared with those in the nontransgenic mice (Fig. 4*b*). The volume density, the most reliable parameter of peroxisome proliferation, was increased age-dependently in the transgenic mice, but the degree of the increase was not as prominent as that observed in mice with clofibrate administration (Fig. 4*b*). The finding that only some hepatocytes in the transgenic mice presented a marked peroxisome proliferation (Fig. 4*a*) is noteworthy, since it seems to correlate with the finding that intense expression of the core protein was observed only in particular hepatocytes.[10] These histological analyses reveal that spontaneous, continuous and age-dependent peroxisome proliferation and PPARα activation occur heterogeneously in the transgenic mouse livers, which is different from the response observed in the mice receiving clofibrate treatment.

Appearance of PPARα-, and cyclin D1-positive hepatocytes

We tried to detect abnormal hepatocytes to clarify the mechanism of hepatocarcinogenesis in the transgenic mice. On PPARα immunofluorescence staining, PPARα was primarily detected in the cytoplasm of the nontransgenic mice and the clofibrate-administered mice. Some hepatocytes having nuclei positively stained

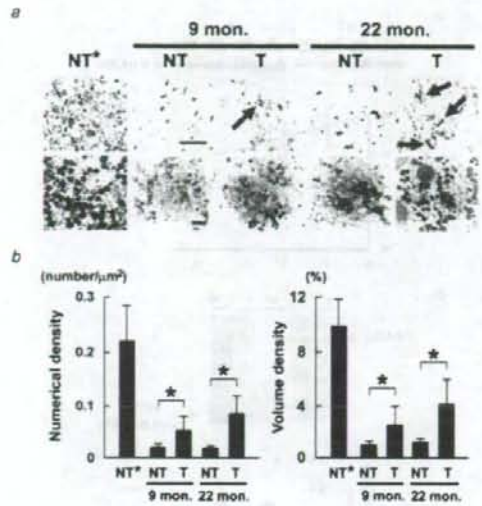

FIGURE 4 – Cytochemical staining for hepatic peroxisomes. (*a*) Light and electron photomicrographs of DAB-stained liver tissues. Peroxisomes are detected as darkly stained particles. The arrows in upper panels indicate hepatocytes showing profound peroxisome proliferation. The bars in the light and electron photomicrographs of 9-month-old nontransgenic mice indicate 50 and 2 μm, respectively. 9 mon, 9-month-old mice; 22 mon, 22-month-old mice; NT, nontransgenic mice; T, transgenic mice; NT*, nontransgenic mice treated with a control diet containing 0.5% clofibrate for 2 weeks. (*b*) Morphometric analysis of hepatic peroxisomes. The number of peroxisomes and the area of each individual peroxisome profile were measured in 10 photomicrographs for each mouse, and morphometric parameters such as numerical density and volume density were calculated. Results are expressed as the mean ± standard deviation ($n = 8$). Abbreviations are identical with those in (*a*). *, $p < 0.05$ between the transgenic mice and the nontransgenic mice.

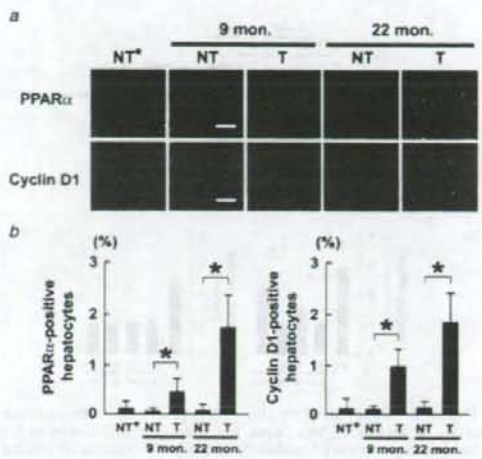

FIGURE 5 – Immunofluorescence staining for PPARα and cyclin D1. (*a*) Immunofluorescence staining using antibodies against PPARα and cyclin D1. The bars in the photomicrographs of 9-month-old nontransgenic mice indicate 50 μm. 9 mon, 9-month-old mice; 22 mon, 22-month-old mice; NT, nontransgenic mice; T, transgenic mice; NT*, nontransgenic mice treated with a control diet containing 0.5% clofibrate for 2 weeks. (*b*) The number of PPARα-, or cyclin D1-positive hepatocytes. Two-thousand hepatocyte nuclei were examined for each mouse, and the number of nuclei intensively stained with anti-PPARα or anti-cyclin D1 antibody was counted. Results are expressed as the mean ± standard deviation ($n = 8$). Abbreviations are identical with those of (*a*). *, $p < 0.05$ between the transgenic mice and the nontransgenic mice.

by anti-PPARα antibody were detected only in the transgenic mice (Fig. 5*a*). Similar to the case of PPARα, the hepatocytes having nuclei stained intensively by anti-cyclin D1 antibody were found only in the transgenic mice (Fig. 5*a*). A few hepatocytes stained by anti-CDK4 antibody were also observed only in the transgenic mice (data not shown). The frequency of appearance of PPARα-, or cyclin D1-positive hepatocytes was increased with age (Figs. 5*a* and 5*b*). Thus, the appearance of these specific hepatocytes in the transgenic mice seemed to be, at least in part, associated with sustained, age-dependent and heterogeneous PPARα activation in the transgenic mice.

Changes in PPARα levels

Since the expression of PPARα is known to be enhanced by its activation,[18,30] the quantitative change in PPARα was evaluated. The nuclear PPARα level in the transgenic mice was increased age-dependently, as expected (Figs. 6*a*, upper panel and 6*b*), but the PPARα level in the whole liver lysate remained unchanged (data not shown). The increase in nuclear PPARα in the transgenic mice was smaller than that in the clofibrate-treated wild-type mice (Figs. 6*a*, upper panel and 6*b*). Northern blot analysis revealed a higher PPARα mRNA level in the clofibrate-treated mice than in the controls, although this parameter in the transgenic mouse groups of each age was similar to that in the controls (Figs. 6*a*, lower panel and 6*b*). These results indicate that the increase in nuclear PPARα in the transgenic mice occurs mainly at the post-transcriptional level, which is distinct from that observed in the clofibrate-treated wild-type mice.

Stabilization of PPARα through a possible interaction with HCV core protein in hepatocyte nuclei

The increased stability of PPARα in hepatocyte nuclei is thought to be one of the possible causes of a disproportional increase in the nuclear PPARα level. To examine this possibility, a pulse-chase experiment was performed using isolated hepatocytes. The half-life of nuclear PPARα was ~7 hr in the control mice and 12.5 hr in the transgenic mice (Fig. 7*a*). In addition, the intensity of the labeled PPARα band (P in Fig. 7*a*, upper panels) in the control mice was similar to that in the transgenic mice. The finding that the [^{35}S]methionine uptake in the hepatocytes from the control mice was similar to that from the transgenic mice suggests that the increase in nuclear PPARα in the hepatocytes from the transgenic mice (Fig. 7*a*, lower right panel), as well as that *in vivo* (Fig. 6*a*, upper panel), is not because of the increased PPARα transfer into the nucleus.

In the transgenic mice, HCV core protein accumulated in the nuclei, as evidenced by immunoelectron microscopy,[11] suggesting a possible interaction of the core protein with PPARα in the nuclei. We therefore examined this possibility by anti-PPARα IgG affinity chromatography. When proteins combining with PPARα in hepatocyte nuclei were subjected to immunoblot analysis, the core protein was clearly detected (Fig. 7*b*). This result suggests the possibility of complex formation between the HCV core protein and PPARα, which is consistent with an interaction of the core protein with retinoid X receptor (RXR) α,[31] an essential heterodimeric partner of PPARα.[32] Thus, HCV core protein may

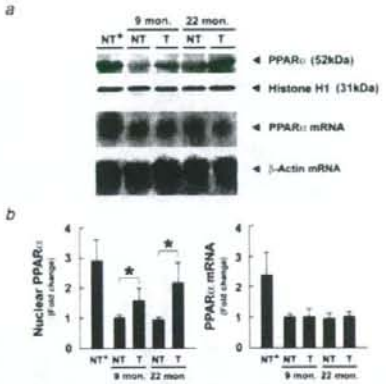

FIGURE 6 – Analysis of PPARα. (*a*) (Upper panels) Immunoblot analysis of nuclear PPARα. Since few individual differences in the same mouse group were found in the preliminary experiments, 30 mg of liver pieces from each mouse ($n = 8$/group) was mixed and homogenized to prepare the nuclear fraction. One-hundred microgram of nuclear protein was separated on 10% SDS-polyacrylamide gel, transferred to nitrocellulose membranes and reacted with antibody against PPARα. The band of histone H1 was used as the loading control. Results are representative of 4 independent experiments. The apparent molecular weight is indicated in parentheses. 9 mon, 9-month-old mice; 22 mon, 22-month-old mice; NT, nontransgenic mice; T, transgenic mice; NT*, nontransgenic mice treated with a control diet containing 0.5% clofibrate for 2 weeks. (Lower panels) Northern blot analysis of PPARα. A sample used in Figure 3*b* was adopted. Hepatic RNA (5 μg) was electrophoresed and hybridized with cDNAs for PPARα and β-actin, respectively. Results are representative of 4 independent experiments. (*b*) Quantification of nuclear PPARα levels and PPARα mRNA levels. The nuclear PPARα level was quantified densitometrically and normalized to the histone H1 level. The mRNA level of PPARα was quantified using a phosphorimager and normalized to that of β-actin. Values were subsequently normalized to those of 9-month-old nontransgenic mice. Results were obtained from 4 independent experiments and expressed as the mean ± standard deviation. Abbreviations are identical with those in (*a*). *, $p < 0.05$ between the transgenic mice and the nontransgenic mice.

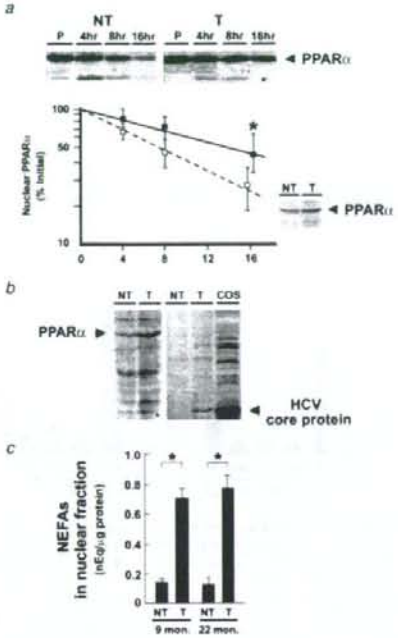

FIGURE 7 – Analyses of PPARα stability, interaction between PPARα with the core protein in hepatocyte nuclei, and nuclear contents of NEFAs. (*a*) Pulse-label and pulse-chase experiments for nuclear PPARα using isolated mouse hepatocytes. (Upper panels) Labeled PPARα bands on X-ray film. Pulse-label and pulse-chase experiments were performed as described in the Material and methods. NT, nontransgenic mice; T, transgenic mice; P, pulse-label; 4, 8, 16 hr, pulse-chase for 4, 8, 16 hr, respectively. (Lower left panel) Intensity plot of PPARα in 5 independent experiments. Values are normalized as a percentage of the values of the pulse-labeled band and expressed as the mean ± standard deviation. Open square, nontransgenic mice; black square, transgenic mice; *, $p < 0.05$ between the transgenic mice and the nontransgenic mice. (Lower right panel) Immunoblot analysis of an isolated hepatocyte nuclear fraction. NT, nontransgenic mice; T, transgenic mice. (*b*) Interaction between PPARα and HCV core protein in the nucleus. (Left panel) Immunoblot analysis (PPARα) of the eluate on anti-PPARα IgG affinity column chromatography. (Right panel) Immunoblot analysis (HCV core protein) of the same eluate. NT, nontransgenic mice; T, transgenic mice; COS, HCV core protein-overexpressing COS cell lysate. (*c*) Nuclear contents of NEFAs. The levels of NEFAs were measured using a hepatocyte nuclear fraction. Results are expressed as the mean ± standard deviation ($n = 8$). *, $p < 0.05$ between the transgenic mice and the nontransgenic mice; NT, nontransgenic mice; T, transgenic mice; 9 mon, 9-month-old mice; 22 mon, 22-month-old mice.

directly or indirectly affect the stability of PPARα in hepatocyte nuclei.

Increase in PPARα ligands

PPARα is a ligand-activated transcription factor. Since the transgenic mice were fed a standard laboratory chow, endogenous substances such as NEFAs would serve as ligands of PPARα[33]; therefore, the contents of NEFAs in hepatocyte nuclei were compared between the 2 groups. The levels of NEFAs in hepatocyte nuclei in the transgenic mice were ~5 times higher than those in the control mice at the same age (Fig. 7*c*). This could account for the higher activation of PPARα in the transgenic mice than in the controls.

Discussion

A large number of variables are involved in the induction of HCC by HCV core protein. While the precise mechanism underlying hepatocarcinogenesis in HCV core gene transgenic mice cannot be fully elucidated from this study, our results could provide some clues to explain this phenomenon. We found spontaneous, persistent, age-dependent and heterogeneous PPARα activation in the transgenic mouse livers for the first time. This study thus advances our understanding of the association between HCV core protein-mediated hepatocarcinogenesis and persistent PPARα activation.

Hepatocyte proliferation is influenced by various factors, such as mitogenic chemicals, cytokines, growth factors and transcription factors. It has been reported that various kinds of cell-cycle regulators and oncogene products are induced by PPARα activation.[19,26–30] In particular, cyclin D1, CDK4, PCNA and c-Myc are potent and critical regulators of the G1-S checkpoint and cell-cycle progression,[13,14] and aberrant expression of these proteins is frequently detected in HCV-related HCC.[34–37] These key regulators are known to be induced in a PPARα-dependent manner in mice[19,30]; the continuous induction of these proteins and the

resultant acceleration of hepatocyte proliferation found in the transgenic mice may be attributed to persistent PPARα activation. In the current study, we demonstrated that there was a great variety of the intensity of PPARα activation among different hepatocytes (Fig. 4). This persistent and heterogeneous PPARα activation found especially in the transgenic mice may be linked with the age-dependent and multicentric hepatocarcinogenesis induced by the core protein.

It is well-known that the long-term administration of potent peroxisome proliferators such as fibrate drugs can induce hepatocarcinogenesis in rodents.[29] The findings observed in the transgenic mice markedly differ from those in mice with long-term treatment of peroxisome proliferators in several ways. Namely, the transgenic mice show no intense increase in AOX and PT (Fig. 3), no increase in PPARα mRNA (Fig. 6), heterogeneous peroxisome proliferation (Fig. 4) and age-dependent emergence of hepatocytes having nuclei stained intensively by anti-PPARα or anti-cyclin D1 antibody (Fig. 5). Therefore, the mode of PPARα activation and the mechanism of hepatocarcinogenesis caused by HCV core protein expression are indeed unique.

One of the mechanisms involved in the core protein-specific PPARα activation in mice is stabilization of PPARα in hepatocyte nuclei through a possible interaction with the core protein. In cultured cells expressing the core protein, it has been demonstrated that the core protein interacts with the PPARα-RXRα heterodimer and enhances the transcriptional activation mediated by PPARα regardless of the presence or absence of its ligands.[31] Since PPARα is ubiquitinated and degraded *via* the proteasome pathway,[38] it may be postulated that HCV core protein directly or indirectly influences the degradation pathway. It has been reported that the core protein binds to the proteasome activator PA28γ[39] which is known to combine with steroid receptor coactivator-3 and to accelerate its degradation.[40] Another possible mechanism is an increase in NEFAs in hepatocyte nuclei. The PPARα activation induced by the core protein enhances the expression of L-FABP,[30] which serves as a transporter of NEFAs into nuclei. Indeed, real-time confocal and multiphoton laser scanning microscopy has shown that L-FABP expression significantly increased the total uptake of medium- and long-chain fluorescent fatty acids into the nuclei of living cells.[41] Thus, increased L-FABP expression may facilitate the shuttling of NEFAs into hepatocyte nuclei for donating NEFAs to PPARα, leading to PPARα activation and further increase in L-FABP expression. Moreover, the binding of ligands causes conformational alternation of PPARα[42] and further stabilizes it in nuclei,[32] resulting in synergistic PPARα activation. Therefore, these findings concerning spontaneous and persistent PPARα activation induced by the core protein enable us to partially explain the precise molecular mechanism of hepatocarcinogenesis in HCV core gene transgenic mice.

The results obtained from the current study are consistent with the findings observed in chronically HCV-infected patients in several ways. That is, like the transgenic mice in the present study, chronically HCV-infected patients have been reported to show accelerated hepatocyte proliferation,[43] an increase in CDK4, cyclin D1 and E, PCNA, c-Myc and c-Fos,[34–37] and multicentric appearance of HCC.[44] Furthermore, it has been reported that a massive proliferation of peroxisomes was found in human nontumorous liver tissue adjacent to HCC.[45] Thus the earlier findings, including the unique function of HCV core protein *in vivo* and the diverse and significant roles of PPARα, may help to partially understand the onset and development of HCC in patients with chronic HCV infection. It has been demonstrated that the function of hepatic PPARα was impaired in patients with chronic HCV infection,[46] which is different from our results. Since HCC had not yet developed in the patients in the report, this discrepancy might derive from differences in the stage of the hepatocarcinogenic process.

The interpretation based on persistent activation of PPARα pertains to only one possible mechanism of hepatocarcinogenesis induced by the effects of HCV core protein. We cannot rule out the presence of other mechanisms. The exact relationship between PPARα activation and hepatocarcinogenesis may be elucidated by additional experiments in which PPARα activation is continuously inhibited in the same transgenic mice. Furthermore, the exact relationship may be confirmed when PPARα-null mice bearing the core protein gene do not represent development of HCC.

In conclusion, we demonstrated for the first time that spontaneous, persistent, age-dependent and heterogeneous activation of PPARα occurred in HCV core protein transgenic mice and caused continuous enhancement of hepatocyte proliferation, which may have contributed to the age-dependent and multicentric hepatocarcinogenesis observed in these mice. In addition, we observed nuclear stabilization of PPARα and an increase in NEFAs in the hepatocyte nuclei of the transgenic mice, which may have resulted in the HCV core protein-specific PPARα activation.

References

1. Kiyosawa K, Tanaka E, Sodeyama T. Hepatitis C virus and hepatocellular carcinoma. In: Reesink HW, ed. Hepatitis C virus: Current Studies in Hematology & Blood Transfusion, vol. 62. Basel: Karger, 1998.161–180.
2. Saito I, Miyamura T, Ohbayashi A, Harada H, Katayama T, Kikuchi S, Watanabe Y, Koi S, Onji M, Ohta Y, Choo QL, Houghton M, et al. Hepatitis C virus infection is associated with the development of hepatocellular carcinoma. Proc Natl Acad Sci USA 1990;87:6547–49.
3. Tanaka Y, Hanada K, Mizokami M, Yeo AE, Shih JW, Gojobori T, Alter HJ. A comparison of the molecular clock of hepatitis C virus in the United States and Japan predicts that hepatocellular carcinoma incidence in the United States will increase over the next two decades. Proc Natl Acad Sci USA 2002;99:15584–89.
4. Kiyosawa K, Umemura T, Ichijo T, Matsumoto A, Yoshizawa K, Gad A, Tanaka E. Hepatocellular carcinoma: recent trends in Japan. Gastroenterology 2004;127:S17–S26.
5. Watashi K, Shimotohno K. The roles of hepatitis C virus proteins in modulation of cellular functions: a novel action mechanism of the HCV core protein on gene regulation by nuclear hormone receptors. Cancer Sci 2003;94:937–43.
6. Ray RB, Lagging LM, Meyer K, Ray R. Hepatitis C virus core protein cooperates with *ras* and transforms primary rat embryo fibroblasts to tumorigenic phenotype. J Virol 1996;70:4438–43.
7. Ray RB, Meyer K, Ray R. Suppression of apoptotic cell death by hepatitis C virus core protein. Virology 1996;226:176–82.
8. McLauchlan J. Properties of the hepatitis C virus core protein: a structural protein that modulates cellular processes. J Viral Hepat 2000; 7:2–14.
9. Tellinghuisen TL, Rice CM. Interaction between hepatitis C virus proteins and host cell factors. Curr Opin Microbiol 2002;5:419–27.
10. Moriya K, Yotsuyanagi H, Shintani Y, Fujie H, Ishibashi K, Matsuura Y, Miyamura T, Koike K. Hepatitis C virus core protein induces hepatic steatosis in transgenic mice. J Gen Virol 1997;78:1527–31.
11. Moriya K, Fujie H, Shintani Y, Yotsuyanagi H, Tsutsumi T, Ishibashi K, Matsuura Y, Kimura S, Miyamura T, Koike K. The core protein of hepatitis C virus induces hepatocellular carcinoma in transgenic mice. Nat Med 1998;4:1065–7.
12. Moriya K, Nakagawa K, Santa T, Shintani Y, Fujie H, Miyoshi H, Tsutsumi T, Miyazawa T, Ishibashi K, Horie T, Imai K, Todoroki T, et al. Oxidative stress in the absence of inflammation in a mouse model for hepatitis C virus-associated hepatocarcinogenesis. Cancer Res 2001;61:4365–70.
13. Sherr CJ. Cancer cell cycles. Science 1996;274:1672–7.
14. Vousden KH, Evan GI. Proliferation, cell cycle and apoptosis in cancer. Nature 2001;411:342–8.
15. Donato MF, Arosio E, Del Ninno E, Ronchi G, Lampertico P, Morabito A, Balestrieri MR, Colombo M. High rates of hepatocellular carcinoma in cirrhotic patients with high liver cell proliferative activity. Hepatology 2001;34:523–8.
16. Yasui K, Wakita T, Tsukiyama-Kohara K, Funahashi S-I, Ichikawa M, Kajita T, Moradpour D, Wands JR, Kohara M. The native form and maturation process of hepatitis C virus core protein. J Virol 1998;72:6048–55.
17. Aoyama T, Peters JM, Iritani N, Nakajima T, Furihata K, Hashimoto T, Gonzalez FJ. Altered constitutive expression of fatty acid-metabo-

lizing enzymes in mice lacking the peroxisome proliferator-activated receptor α (PPARα). J Biol Chem 1998;273:5678–84.
18. Lee SS, Pineau T, Drago J, Lee EJ, Owens JW, Kroetz DL, Fernandez-Salguero PM, Westphal H, Gonzalez FJ. Targeted disruption of the α isoform of the peroxisome proliferator-activated receptor gene in mice results in abolishment of the pleiotropic effects of peroxisome proliferators. Mol Cell Biol 1995;15:3012–22.
19. Peters JM, Aoyama T, Cattley RC, Nobumitsu U, Hashimoto T, Gonzalez FJ. Role of peroxisome proliferator-activated receptor α in altered cell cycle regulation in mouse liver. Carcinogenesis 1998; 19:1989–94.
20. Ni R, Tomita Y, Matsuda K, Ichihara A, Ishimura K, Ogasawara J, Nagata S. Fas-mediated apoptosis in primary cultured mouse hepatocytes. Exp Cell Res 1994;215:332–7.
21. Harada S, Watanabe Y, Takeuchi K, Suzuki T, Katayama T, Takebe Y, Saito I, Miyamura T. Expression of processed core protein of hepatitis C virus in mammalian cells. J Virol 1991;65:3015–21.
22. Novikoff AB, Goldfischer S. Visualization of peroxisomes (microbodies) and mitochondria with diaminobenzidine. J Histochem Cytochem 1969;17:675–80.
23. Gurtu V, Kain SR, Zhang G. Fluorometric and colorimetric detection of caspase activity associated with apoptosis. Anal Biochem 1997; 251:98–102.
24. Folch J, Lees M, Sloane Stanley GH. A simple method for the isolation and purification of total lipids from animal tissues. J Biol Chem 1957;226:497–509.
25. Furutani T, Hino K, Okuda M, Gondo T, Nishina S, Kitase A, Korenaga M, Xiao SY, Weinman SA, Lemon SM, Sakaida I, Okita K. Hepatic iron overload induces hepatocellular carcinoma in transgenic mice expressing the hepatitis C virus polyprotein. Gastroenterology 2006;130:2087–98.
26. Cherkaoui-Malki M, Lone YC, Corral-Debrinski M, Latruffe N. Differential proto-oncogene mRNA induction from rats treated with peroxisome proliferators. Biochem Biophys Res Commun 1990; 173:855–61.
27. Ledwith BJ, Johnson TE, Wagner LK, Pauley CJ, Manam S, Galloway SM, Nichols WW. Growth regulation by peroxisome proliferators: opposing activities in early and late G1. Cancer Res 1996; 56:3257–64.
28. Rininger JA, Goldsworthy TL, Babishi JG. Time course comparison of cell-cycle protein expression following partial hepatectomy and WY14,643-induced hepatic cell proliferation in F344 rats. Carcinogenesis 1997;18:935–41.
29. Peters JM, Cheung C, Gonzalez FJ. Peroxisome proliferator-activated receptor-α and liver cancer: where do we stand? J Mol Med 2005; 83:774–85.
30. Mandard S, Muller M, Kersten S. Peroxisome proliferator-activated receptor α target genes. Cell Mol Life Sci 2004;61:393–416.
31. Tsutsumi T, Suzuki T, Shimoike T, Suzuki R, Moriya K, Shintani Y, Fujie H, Matsuura Y, Koike K, Miyamura T. Interacton of hepatitis C virus core protein with retinoid X receptor α modulates its transcriptional activity. Hepatology 2002;35:937–46.
32. Tanaka N, Hora K, Makishima H, Kamijo Y, Kiyosawa K, Gonzalez FJ, Aoyama T. In vivo stabilization of nuclear retinoid X receptor α in the presence of peroxisome proliferator-activated receptor α. FEBS Lett 2003;543:120–4.
33. Desvergne B, Wahli W. Peroxisome proliferator-activated receptors: nuclear control of metabolism. Endocr Rev 1999;20:649–88.
34. Ito Y, Sasaki Y, Horimoto M, Wada S, Tanaka Y, Kasahara A, Ueki T, Hirano T, Yamamoto H, Fujimoto J, Okamoto E, Hayashi N, et al. Activation of mitogen-activated protein kinases/extracellular signal-regulated kinases in human hepatocellular carcinoma. Hepatology 1998;27:951–8.
35. Masaki T, Shiratori Y, Rengifo W, Igarashi K, Yamagata M, Kurokohchi K, Uchida N, Miyauchi Y, Yoshiji H, Watanabe S, Omata M, Kuriyama S. Cyclins and cyclin-dependent kinases: comparative study of hepatocellular carcinoma versus cirrhosis. Hepatology 2003;37:534–43.
36. Nardone G, Romano M, Calabro A, Pedone PV, de Sio I, Persico M, Budillon G, Bruni CB, Riccio A, Zarrilli R. Activation of fetal promoters of insulin-like growth factors II gene in hepatitis C virus-related chronic hepatitis, cirrhosis, and hepatocellular carcinoma. Hepatology 1996;23:1304–12.
37. Kawate S, Fukusato T, Ohwada S, Watanuki A, Morishita Y. Amplification of *c-myc* in hepatocellular carcinoma: correlation with clinicopathologic features, proliferative activity and p53 overexpression. Oncology 1999;57:157–63.
38. Genini D, Catapano CV. Control of peroxisome proliferator-activated receptor fate by the ubiquitin-proteasome system. J Recept Signal Transduct Res 2006;26:679–92.
39. Moriishi K, Okabayashi T, Nakai K, Moriya K, Koike K, Murata S, Chiba T, Tanaka K, Suzuki R, Suzuki T, Miyamura T, Matsuura Y. Proteasome activator PA28γ-dependent nuclear retention and degradation of hepatitis C virus core protein. J Virol 2003;77:10237–49.
40. Li X, Lonard D, Jung SY, Malovannaya A, Feng Q, Qin J, Tsai SY, Tsai M, O'Malley BW. The SRC-3/AIB1 coactivator is degraded in a ubiquitin- and ATP-independent manner by the REGγ proteasome. Cell 2006;124:381–92.
41. Huang H, Starodub O, McIntosh A, Kier AB, Schroeder F. Liver fatty acid-binding protein targets fatty acids to the nucleus. Real time confocal and multiphoton fluorescence imaging in living cells. J Biol Chem 2002;277:29139–51.
42. Dowell P, Peterson VJ, Zabriskie TM, Leid M. Ligand-induced peroxisome proliferator-activated receptor α conformational change. J Biol Chem 1997;272:2013–20.
43. Farinati F, Cardin R, Fiorentino M, D'Errico A, Grigioni W, Cecchetto A, Naccarato R. Imbalance between cytoproliferation and apoptosis in hepatitis C virus related chronic liver disease. J Viral Hepat 2001;8:34–40.
44. Oikawa T, Ojima H, Yamasaki S, Takayama T, Hirohashi S, Sakamoto M. Multistep and multicentric development of hepatocellular carcinoma: histological analysis of 980 resected nodules. J Hepatol 2005;42:225–9.
45. Litwin JA, Beier K, Volkl A, Hofmann WJ, Fahimi HD. Immunocytochemical investigation of catalase and peroxisomal lipid β-oxidation enzymes in human hepatocellular tumors and liver cirrhosis. Virchows Arch 1999;435:486–95.
46. Dharancy S, Malapel M, Perlemuter G, Roskams T, Cheng Y, Dubuquoy L, Podevin P, Conti F, Canva V, Philippe D, Gambiez L, Mathurin P, et al. Impaired expression of the peroxisome proliferator-activated receptor α during hepatitis C virus infection. Gastroenterology 2005;128:334–2.

J Gastroenterol 2009; 44[Suppl XIX]:82–88
DOI 10.1007/s00535-008-2276-4

Journal of Gastroenterology

Steatosis, liver injury, and hepatocarcinogenesis in hepatitis C viral infection

Kazuhiko Koike

Department of Infectious Diseases, Internal Medicine, Graduate School of Medicine, University of Tokyo, 7-3-1 Hongo, Bunkyo-ku, Tokyo 113-8655, Japan

In addition to the link with development of hepatocellular carcinoma (HCC), hepatitis C virus (HCV) infection is associated with several hepatic and extrahepatic manifestations. A role of hepatic steatosis in the pathogenesis of chronic hepatitis C has been shown, implying hepatitis C as a metabolic disease. Furthermore, recent epidemiological studies have suggested a linkage between insulin resistance and chronic HCV infection. In addition to the data indicating the presence of lipid metabolism disturbance and insulin resistance in the cohort of chronic hepatitis C patients, we found evidence showing the association between these two conditions and HCV infection using mice transgenic for the HCV core gene. These mice develop HCC late in life after the phase of hepatic steatosis and insulin resistance. The nonappearance of both steatosis and HCC in HCV core gene transgenic mice that are null for the proteasome activator 28γ implies a close relationship between lipid metabolism disturbance and hepatocarcinogenesis. Also, the core protein is shown to bind with retinoid X receptor (RXR)-α, resulting in the upregulation of some lipid metabolism enzymes, including cellular retinol binding protein II and acyl-CoA oxidase. In addition, the persistent activation of peroxisome proliferator activated receptor (PPAR)-α has recently been found in the liver of HCV core gene transgenic mice, yielding dramatic changes in lipid metabolism and hepatocyte proliferation, including HCC development. These results would provide a clue for further understanding of the role of lipid metabolism in pathogenesis of HCV infection, including liver injury and hepatocarcinogenesis.

Received: June 9, 2008 / Accepted: August 10, 2008
Reprint requests to: K. Koike

Key words: lipid metabolism, transgenic mouse, oxidative stress, intracellular signal transduction, peroxisome proliferator activated receptor

Introduction

Worldwide, approximately 170 million people are persistently infected with hepatitis C virus (HCV), which induces a spectrum of chronic liver diseases from chronic hepatitis to cirrhosis and, eventually, to hepatocellular carcinoma (HCC).[1] HCV has been given increasing attention because of its wide and deep penetration in the community, tied with a very high incidence of HCC in persistent HCV infection. Once liver cirrhosis is established in hosts persistently infected with HCV, HCC develops at a yearly rate of approximately 7%,[2] resulting in the development of HCC in nearly 90% of HCV-associated cirrhotic patients in 15 years. In addition, the outstanding features in the mode of hepatocarcinogenesis in HCV infection, i.e., development of HCC in a multicentric fashion and at a very high incidence, are not common in other malignancies except for hereditary cancers such as familial polyposis of the colon. Knowledge of the mechanism underlying HCC development in persistent HCV infection, therefore, is imminently required for the prevention of HCC.

In addition to the link with development of HCC, HCV infection is associated with several hepatic and extrahepatic manifestations.[3] A role of hepatic steatosis in the pathogenesis of chronic hepatitis C has been shown, implicating hepatitis C as a metabolic disease.[4] Moreover, recent epidemiological studies have suggested a linkage between insulin resistance and chronic HCV infection.[5] In addition to the epidemiological data indicating the presence of lipid metabolism disturbance and insulin resistance in the cohort of chronic hepatitis C patients, detailed analyses on the relationship between

metabolic disorders and chronic hepatitis C have revealed evidence showing a close association between the progression of liver fibrosis and metabolic abnormalities in HCV infection.[6] However, it is unclear yet whether a causative relationship exists between these medical conditions. Moreover, it is unclear whether such metabolic disorders contribute to hepatocarcinogenesis in HCV infection.

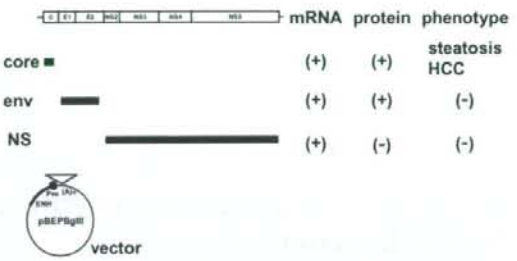

Fig. 1. Transgenic mouse lines carrying the hepatitis C virus (HCV) genome. Three different kinds of transgenic mouse lines, carrying the *core* gene, envelope genes, or nonstructural genes of HCV, respectively, were established under the control of the same regulatory elements. Among these mouse strains, only the transgenic mice carrying the HCV core gene develop hepatocellular carcinoma (HCC) after an early phase with hepatic steatosis in two independent lineages. The mice transgenic for the envelope genes or nonstructural genes do not develop HCC. *HCC*, hepatocellular carcinoma; *env*, envelope genes; *NS*, nonstructural genes

Possible roles of HCV in hepatocarcinogenesis

The mechanism underlying hepatocarcinogenesis in HCV infection is not yet fully understood, despite the fact that nearly 80% of patients with HCC in Japan are persistently infected with HCV.[1,7,8] HCV infection is also common in patients with HCC in other countries, albeit to a lesser extent. These lines of evidence prompted us to seek to determine the role of HCV in hepatocarcinogenesis. Inflammation induced by HCV should be considered, of course, in a study on the hepatocarcinogenesis in hepatitis viral infection: necrosis of hepatocytes caused by chronic inflammation followed by regeneration enhances genetic aberrations in host cells, the accumulation of which culminates in HCC. This theory presupposes an indirect involvement of hepatitis viruses in HCC via hepatic inflammation. However, this context leaves us with a serious question: can inflammation alone result in the development of HCC in such a high incidence (90% in 15 years) or multicentric nature in HCV infection?

The other role of HCV would have to be weighed against an extremely rare occurrence of HCC in patients with autoimmune hepatitis in which severe inflammation in the liver persists indefinitely, even after the development of cirrhosis. This background and reasoning lead to a possible activity of viral proteins for inducing neoplasia. This possibility has been evaluated by introducing genes of HCV into hepatocytes in culture with little success. One of the difficulties in using cultured cells is the carcinogenic capacity of HCV, if any, which would be weak and would take a long time to manifest. Actually, it takes 30–40 years for HCC to develop in individuals infected with HCV. On the basis of these points of view, we started to investigate carcinogenesis in chronic hepatitis C, in vivo, by transgenic mouse technology.

HCV core protein has an in vivo oncogenic activity as revealed by animal studies

Transgenic mouse lines carrying the HCV genome were engineered by introducing the genes from the cDNA of the HCV genome of genotype 1b.[9,10] Established are three different kinds of transgenic mouse lines, which carry the core gene, envelope genes, or nonstructural genes, respectively, under the same transcriptional regulatory element. Among these mouse lines, only the transgenic mice carrying the core gene developed HCC in two independent lineages.[10] The envelope gene transgenic mice do not develop HCC, despite high expression levels of both E1 and E2 proteins,[11,12] and the transgenic mice carrying the entire nonstructural genes have developed no HCC (Fig. 1).

The core gene transgenic mice express the core protein of an expected size, and the level of the core protein in the liver is similar to that in chronic hepatitis C patients. Early in life, these mice develop hepatic steatosis, which is one of the histological characteristics of chronic hepatitis C, along with lymphoid follicle formation and bile duct damage.[13] Thus, the core gene transgenic mouse model reproduces well the features of chronic hepatitis C. Of note, no pictures of significant inflammation are observed in the liver of this animal model. Late in life, these transgenic mice develop HCC. Notably, the development of steatosis and HCC has been reproduced by other HCV transgenic mouse lines, which harbor the entire HCV genome or structural genes including the core gene.[14–16] These outcomes indicate that the core protein, per se, of HCV has an oncogenic potential when expressed in vivo.

Oxidative stress overproduction and intracellular signaling pathway activation are the major pathways in the core-induced liver pathology

It is difficult to elucidate the mechanism underlying the development of HCC, even for our simple model in which only the core protein is expressed in otherwise normal liver. There is a notable feature in the localization of the core protein in hepatocytes; while the core protein predominantly exists in the cytoplasm associated with lipid droplets, it is also present in the mitochondria and nuclei.[10,17] On the basis of this finding, the pathways related to these two organelles, the mitochondria and nuclei, were thoroughly investigated.

One effect of the core protein is an increased production of oxidative stress in the liver. We would like to draw particular attention to the fact that the production of oxidative stress is increased in our transgenic mouse model in the absence of inflammation in the liver. This finding reflects a state of overproduction of reactive oxygen species (ROS) in the liver,[18] or predisposition to it, which is staged by the HCV core protein without any intervening inflammation.[19,20] The overproduction of oxidative stress results in the generation of deletions in mitochondrial and nuclear DNA, an indicator of genetic damage. In addition, analysis of antioxidant system revealed that some antioxidative molecules are not increased despite the overproduction of ROS in the liver of core gene transgenic mice: hemeoxygenase-1 and glutathione peroxidase are not augmented whereas catalase and glutathione S-transferase levels are increased and enhanced by iron overloading (Moriya et al., manuscript in preparation). These results suggest that HCV core protein not only induces overproduction of ROS but also attenuates some of the antioxidant systems, which may explain the mechanism underlying the production of a strong oxidative stress in HCV infection compared to other forms of hepatitis.

In the absence of inflammation, thus, the core protein induces oxidative stress overproduction, which may, at least in part, contribute to hepatocarcinogenesis in HCV infection. If inflammation were added to the liver with the HCV core protein, the production of oxidative stress would be escalated to an extent that can no longer be scavenged by a physiological antagonistic system. This idea suggests that the inflammation in chronic HCV infection would have a characteristic difference in its quality from those of other types of hepatitis, such as autoimmune hepatitis. The basis for the overproduction of oxidative stress may be ascribed to the mitochondrial dysfunction.[10,19] The dysfunction of the electron transfer system of the mitochondrion is suggested in association with the presence of the HCV core protein.[21]

Other pathways in hepatocarcinogenesis would be the alteration of the expression of cellular genes and modulation of intracellular signaling pathways. For example, tumor necrosis factor (TNF)-α and interleukin-1β have been found to be transcriptionally activated.[22] The mitogen-activated protein kinase (MAPK) cascade is also activated in the liver of the core gene transgenic mouse model. The MAPK pathway, which consists of three routes, c-Jun N-terminal kinase (JNK), p38, and extracellular signal-regulated kinase (ERK), is involved in numerous cellular events including cell proliferation. In the liver of the core gene transgenic mouse model before HCC development, only the JNK route is activated. Downstream of JNK activation, transcription factor activating protein (AP)-1 activation is markedly enhanced.[20,21] At far downstream, both the mRNA and protein levels of cyclin D1 and CDK4 are increased. Thus, the HCV core protein modulates the intracellular signaling pathways and gives an advantage for cell proliferation to the hepatocytes. Interestingly, we found recently that a protein interacting with the core protein, proteasome activator 28γ (PA28γ), is indispensable for the core protein to exert its function for the development of steatosis, insulin resistance, and HCC.[23,24]

Lipid metabolism and HCV infection

Steatosis is frequently observed in chronic hepatitis C patients and is significantly associated with increased fibrosis and progression rate of fibrosis of the liver.[6] A comprehensive analysis of gene expression in the liver of core gene transgenic mice, in which steatosis develops from early in life, revealed that a number of genes related to lipid metabolism are significantly upregulated or downregulated (Table 1).

The composition of fatty acids that are accumulated in the liver of core gene transgenic mice is different from that in fatty liver resulting from simple obesity. Carbon-18 monounsaturated fatty acids (C18:1) such as oleic or vaccenic acids are significantly increased; this is also the case in the comparison of liver tissues from hepatitis C patients and patients with simple fatty liver due to obesity.[20] The mechanism of steatogenesis in hepatitis C was investigated using this mouse model. There are at least three pathways for the development of steatosis. One is the frequent presence of insulin resistance in hepatitis C patients as well as in the core gene transgenic mice, which occurs through the inhibition of tyrosine phosphorylation of insulin receptor substrate (IRS)-1.[25] Insulin resistance increases the peripheral release and hepatic uptake of fatty acids, resulting in an accumulation of lipid in the liver. The second pathway is the suppression of the activity of